

General Disclaimer

One or more of the Following Statements may affect this Document

- This document has been reproduced from the best copy furnished by the organizational source. It is being released in the interest of making available as much information as possible.
- This document may contain data, which exceeds the sheet parameters. It was furnished in this condition by the organizational source and is the best copy available.
- This document may contain tone-on-tone or color graphs, charts and/or pictures, which have been reproduced in black and white.
- This document is paginated as submitted by the original source.
- Portions of this document are not fully legible due to the historical nature of some of the material. However, it is the best reproduction available from the original submission.

(NASA-CR-135367) COMPUTER-AIDED ANALYSIS
AND DESIGN OF THE SHAPE ROLLING PROCESS FOR
PRODUCING TURBINE ENGINE AIRFOILS Interim
Topical Report, 1 Oct. 1976 - 31 Dec. 1977
(Battelle Columbus Labs., Ohio.) 65 p

N79-26175

G3/26

Unclas
27849

4/78
R-0 5-78
367 6-78
8-78
10-78
12-78
6-79
7-79



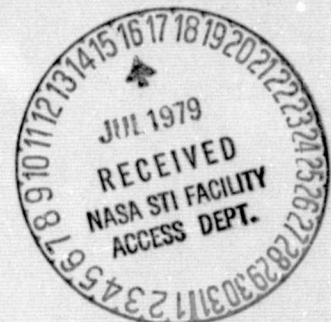
**Computer-Aided Analysis and Design of the Shape Rolling
Process for Producing Turbine Engine Airfoils**

G. D. Lahoti, N. Akgerman, and T. Altan

March, 1978

BATTELLE
Columbus Laboratories
505 King Avenue
Columbus, Ohio 43201

prepared for



NATIONAL AERONAUTICS AND SPACE ADMINISTRATION

NASA Lewis Research Center

Contract NAS 3-20380

Interim Topical Report

COMPUTER-AIDED ANALYSIS AND DESIGN OF THE SHAPE ROLLING PROCESS
FOR PRODUCING TURBINE ENGINE AIRFOILS

G. D. Lahoti, N. Akgerman and T. Altan

March 1978

BATTELLE
Columbus Laboratories
505 King Avenue
Columbus, Ohio 43201

Prepared for

NATIONAL AERONAUTICS AND SPACE ADMINISTRATION

NASA-LEWIS RESEARCH CENTER

Contract NAS3-20380

INTERIM TOPICAL REPORT

FOREWORD

This Interim Topical Report on "Computer-Aided Analysis and Design of the Shape-Rolling Process for Producing Turbine Engine Airfoils" is prepared for NASA Lewis Research Center and covers the work performed under Contract No. NAS3-20380, with Battelle's Columbus Laboratories, from October 1, 1976, to December 31, 1977. The Technical Monitor for this program is Dr. J. Whittenberger, Materials Application Branch, NASA Lewis Research Center, Cleveland, Ohio 44135.

This program is being conducted at Battelle in the Metalworking Section, with Mr. T. G. Byrer as Section Manager. Drs. G. D. Lahoti and N. Akgerman are the principal investigators of the program and, at Battelle, the work is being technically directed by Dr. T. Altan, Research Leader. Other members of Battelle staff are being consulted, as necessary. The experimental work under this program is being recorded in Battelle's Laboratory Record Book No. 33670.

SUMMARY

A computer-aided design (CAD) system has been developed. This system consists of (a) a mathematical model for predicting metal flow (elongation and spread) in shape rolling, and (b) a model for estimating stresses in rolling and for simulating the rolling process. These models utilize the upper-bound method and the slab method of analysis, respectively. This CAD system requires information on material flow stress and workability and information on interface friction as inputs. The predictions from the CAD system are being verified with respect to cold and hot-isothermal rolling of an airfoil shape.

This progress report covers (a) the determination of the flow stress, friction and workability data, (b) the development of the CAD system for rolling of airfoil shapes, (c) the evaluation of the CAD system using plate rolling experiments, and (d) an outline of the shape-rolling experiments to be conducted. A Final Report will be issued upon completion of this program.

TABLE OF CONTENTS

	<u>Page</u>
INTRODUCTION	1
OUTLINE OF PROGRAM	1
BACKGROUND ON SHAPE ROLLING.	2
DETERMINATION OF FLOW STRESS, WORKABILITY AND FRICTION FACTOR.	9
MATERIAL DEFORMATION STUDIES	12
Materials	12
Flow Stress	12
Workability	23
Friction Factor	24
ANALYSIS AND PREDICTION OF METAL FLOW.	24
MODELING FOR LOAD AND STRESS ANALYSIS.	36
EXPERIMENTAL EVALUATION OF COMPUTER MODELS	43
Plate-Rolling Experiments	45
Shape-Rolling Experiments	48
SUMMARY OF RESULTS AND FUTURE WORK	55
REFERENCES	56
DISTRIBUTION LIST.	58

LIST OF ILLUSTRATIONS

Figure No.

1. Three Types of Metal Flow in Rolling of Shapes.	4
2. Analysis of a Roll Pass Used in Rolling Rails ⁽⁵⁾	5
3. Schematic of Five Different Roll-Pass Designs for an Angle Shape from Steel ⁽⁶⁾	5
4. Schematic of Two Different Roll-Pass Designs for a Steel Angle with Unequal Legs ⁽⁷⁾	7
5. Nonuniform Deformation in Rolling of a Shape.	8
6. Metal Flow in Ring Compression Test	10

LIST OF ILLUSTRATIONS (Continued)

<u>Figure No.</u>	<u>Page</u>
7. Experimental Set Up on a Universal Testing Machine for Hot Upset Tests	16
8. Uniform Compression Test Results for AISI 1015 at Room Temperature.	17
9. Uniform Compression Test Results for INCO 718 at Room Temperature .	18
10. Uniform Compression Test Results for Ti-6Al-4V at 927 C (1700 F). .	19
11. Photomicrographs of As-Received Ti-6Al-4V	20
12. Photomicrographs of Heat-Treated Ti-6Al-4V.	21
13. Photomicrographs of Test Specimen after Compression Test.	22
14. Deformed Samples from Nonuniform Compression Tests for Determining Workability	23
15. Theoretical Calibration Curves and Experimental Points for Determining Friction from Upsetting 6:3:2 Rings	25
16. AISI 1015 Rings before and after Deformation.	26
17. Configuration of Deformation Zone in Rolling of Airfoil Shapes. . .	28
18. Division of an Airfoil Section into Rectangular Elements.	30
19. Configuration of an Element in the x-y and x-z Planes	31
20. Rolling of GE's H-369 Airfoil from Mild Steel Using 203.2 mm Rolls	35
21. Stresses in Plane-Strain Upsetting Between Inclined Plates and with Unit Depths.	38
22. Deformation of a Preform as it Enters Airfoil Shaped Rolls. The Stress Outline is Labeled as Step 1 in Figure 24.	40
23. Rolled Airfoil as it Exits the Rolls. The Calculated Stress Distribution is Displayed at Step 15 of Figure 24	41
24. Three-Dimensional Representation of the Calculated Stress (σ_z) Surface for Rolling of the Shape Illustrated in Figure 22	42
25. Plan and Side Views of Theoretical Contact Area of Rolls and Material During Rolling of Airfoils	44
26. Theoretically Predicted and Experimentally Measured Roll-Separating Force for Room Temperature Rolling of 1-Inch Thick Mild Steel Plates of Various Aspect Ratio W_o/H_o (Width/Thickness) .	46

LIST OF ILLUSTRATIONS (Continued)

<u>Figure No.</u>	<u>Page</u>
27. Theoretically Predicted and Experimentally Measured Roll Torque for Room Temperature Rolling of 1-Inch Thick Mild Steel Plates for Various Width to Thickness Ratios (W_0/H_0)	47
28. Theoretically Predicted and Experimentally Measured Roll Torque in Cold Rolling of Mild Steel Plates.	49
29. Theoretically Predicted and Experimentally Measured Roll Torque in Cold Rolling of Mild Steel Plates.	50
30. The Enlarged Sketch of the GE Vane Shape, Which is Being Commercially Rolled from INCO 718 by GE-Lynn.	51
31. Exit End of 2-Hi Rolling Mill for Isothermal Shape-Rolling Trials .	53
32. Roll Assembly for Rolling of Airfoil Shapes	54

INTRODUCTION

Rolling of shapes is one of the least understood metal-deformation processes. A round or round-cornered rectangular bar is rolled in several passes into a nonsymmetric shape, such as L, U, T, I, H, or an airfoil. During each pass, the bar elongates as well as spreads. Thus, a very complex three-dimensional metal flow takes place. The spread is usually only a small fraction of the elongation. However, the ratio between spread and elongation varies at each pass with reduction, roll-shape configuration, bar material and temperature, friction between the rolls and the bar, roll speed, roll diameter, and roll surface finish. The factors influencing the process of rolling a shape are so intermixed and complex that roll and roll-pass design have been, until now, a purely empirical, intuitive, and experience-based art. Through decades of experience, roll-pass designs have been developed for most commonly used shapes from conventional materials. However, when novel processes, such as the high-temperature rolling process, and relatively new materials, such as titanium and nickel alloys, are used, the empirical rules do not directly apply. Process development through experimentation becomes very time consuming and expensive. Consequently, it is necessary to develop objective and quantitative engineering methods for roll-pass design. Since, in shape rolling, there are large numbers of process variables involved, and since the complex metal flow is difficult to analyze, the use of computer techniques as an engineering tool becomes extremely attractive and practical.

OUTLINE OF PROGRAM

The purpose of the present program is to develop and verify a method for computer-aided analysis of the shape-rolling process with emphasis on turbine-engine airfoil geometries. Computerized models are to be developed to analyze the mechanics of metal deformation during rolling of complex geometries, such as airfoils, and to predict the roll-pass design requirements. Evaluation of the models will be accomplished by conducting laboratory rolling experiments of an airfoil shape using the predictions of the computer models. In addition, the computerized models will be applied to at least one commercial airfoil or similar shape-rolling process that is currently in production. A comparison of

experimental results with predicted values will be made along with corrections to the models as required to improve predictability. Finally, the cost benefits of applying computer-aided analyses to shape rolling and to at least two other metal-forming processes are to be determined.

Computer models of materials deformation mechanics in shape rolling were developed using the upper-bound method and the slab method. Computer model for roll-pass design for rolling airfoil shapes was developed based on mechanics models. For experimental evaluation of these models, laboratory rolling experiments will be conducted using AISI 1018 steel as model cold-rolling material and Ti-6Al-4V alloy as a typical hot-rolling material. INCONEL 718 (INCO 718) was selected as a material currently being used in cold rolling of airfoil shapes.

This is an Interim Report and work accomplished to date includes the following:

- (a) Determination of flow stress, friction and workability data
- (b) Development of a CAD system for deformation mechanics of shape rolling and for roll-pass design in rolling of airfoil shapes
- (c) Evaluation of the CAD system using plate-rolling experiments

The future work will consist of conducting cold and hot-isothermal rolling trials, evaluating the CAD system, and developing a cost-benefit analysis of using CAD in metal-forming process design.

BACKGROUND ON SHAPE ROLLING

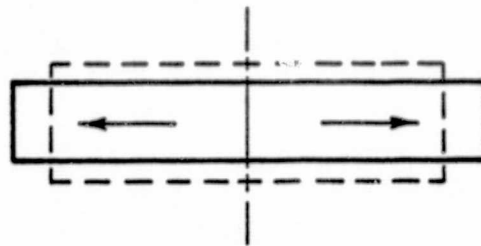
Shape rolling is a relatively old and well-known process and the expenditures involved in establishing a shape-rolling installation are in the order of several million dollars. The costs of designing and manufacturing of rolls for a given shape are very high. Despite these factors, however, there are very little useful, quantitative engineering data on shape rolling available in the published literature⁽¹⁻³⁾. A relatively recent book, published in East Germany, summarizes the advances made in roll-pass design in the Eastern and Western rolling industry and research laboratories⁽⁴⁾. Although several empirical engineering methods are

available for estimating the roll-separating force and the roll torque in shape rolling, it appears that, until today, no quantitative engineering method of analyzing the complex three-dimensional deformation and of roll-pass design exists.

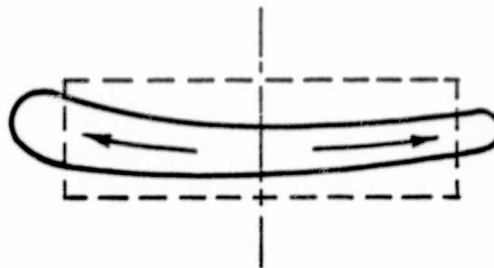
Metal Flow in Shape Rolling. In terms of complexity of metal flow, the shape-rolling process can be classified in the following three categories:

- (a) Uniform Reduction of Cross Section: This type of deformation occurs in rolling of thick plates. The material elongates in the longitudinal direction and spreads in the transverse direction while it is compressed uniformly in the thickness direction. This is illustrated schematically in Figure 1a.
- (b) Moderately Nonuniform Reduction of Cross Section: Rolling of an oval shape or an airfoil section from a rectangular cross section, as shown in Figure 1b, can be considered in this category. Here, the reduction in the thickness direction is nonuniform. However, the metal elongates and spreads laterally outwards in a manner similar to that in rolling of plates.
- (c) Highly Nonuniform Reduction of Cross Section: In this type of deformation, the reduction is highly nonuniform in thickness direction, and part of the cross section is reduced in height while other parts may be extruded, as shown in Figure 1c. This results in both inward and outward flow of metal in the lateral direction and a flow perpendicular to the plane of rolling. In addition, the metal flows in the longitudinal direction.

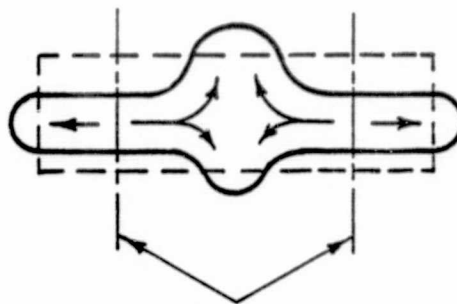
The lateral metal flow, briefly discussed above, must be quantitatively evaluated for each pass within the deformation zone between the rolls. The deformation zone is limited with the entrance, where an already prerolled shape enters the rolls, and the exit, where the rolled shape leaves the rolls. A method for investigating the metal flow in shape rolling is illustrated in Figure 2⁽⁵⁾. The deformation zone is cross sectioned with several planes, 1



(a)



(b)



Neutral planes

(c)

FIGURE 1. THREE TYPES OF METAL FLOW IN ROLLING OF SHAPES

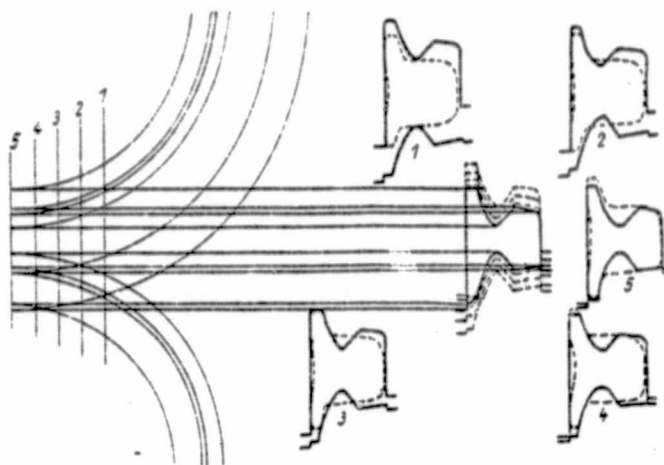


FIGURE 2. ANALYSIS OF A ROLL PASS USED IN ROLLING RAILS⁽⁵⁾
 (Sketches 1 through 5 illustrate the stock, broken lines and the roll, full lines at various positions of the deformation zone)

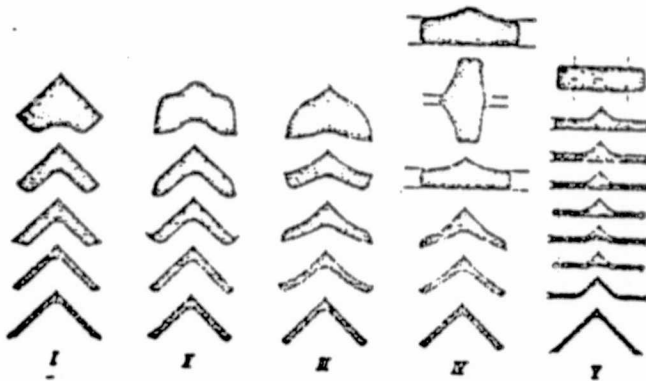


FIGURE 3. SCHEMATIC OF FIVE DIFFERENT ROLL-PASS⁽⁶⁾
 DESIGNS FOR AN ANGLE SHAPE FROM STEEL

ORIGINAL PAGE IS
 OF POOR QUALITY

through 5, (1 is at entrance, 5 is at exit). The roll position and the deformation of the incoming billet are investigated at each of these planes. Thus, a more detailed analysis of metal flow and an improved method for designing the configuration of the rolls is possible. It is evident that this technique can be drastically improved and made extremely efficient by using a computer. The computer, then, would allow to take a very large number of cross-sectional planes and would automatically draft the configurations of the rolls and of the billet at each cross section.

Roll-Pass Design. For a given material and final cross-sectional shape, there is no unique method of roll-pass design. For example, Figure 3 illustrates schematically five different methods of pass design for a steel angle with equal legs⁽⁶⁾. Similar illustrations are given in Figure 4 for a steel angle with unequal legs.

In roll-pass design for shapes, the most difficult problem is due to the fact that the cross section of a shape is not deformed uniformly. This is illustrated in Figure 5 for a relatively simple shape. The reductions in height are not equal for the Zones A and B of the shape, seen in Figure 5a. Consequently, if these two Zones, A and B, were completely independent from each other, Figure 5b, the Zone B would elongate much longer than the Zone A. However, both zones are connected and as part of rolled shape, they must have equal elongation at the exit from the rolls. Therefore, during rolling, metal must flow from Zone B into Zone A so that a uniform elongation of the overall cross section is obtained⁽⁷⁻⁹⁾. This lateral flow is also influenced by the temperature differences which exist in the cross section because of varying material thickness and heat flow.

In establishing the number of passes and the shape of the rolls for each pass, the following factors must be considered:

- (1) The Characteristics of the Available Installation: These include: (a) diameters and lengths of the rolls, (b) bar dimensions, (c) distance between roll stands, (d) distance from last stand to the shear, and (e) tolerances which are required and which can be maintained.
- (2) Reduction per Pass: The reduction per pass must be so large that (a) the installation is utilized at a maximum capacity, (b) the roll stands must not be overloaded, and

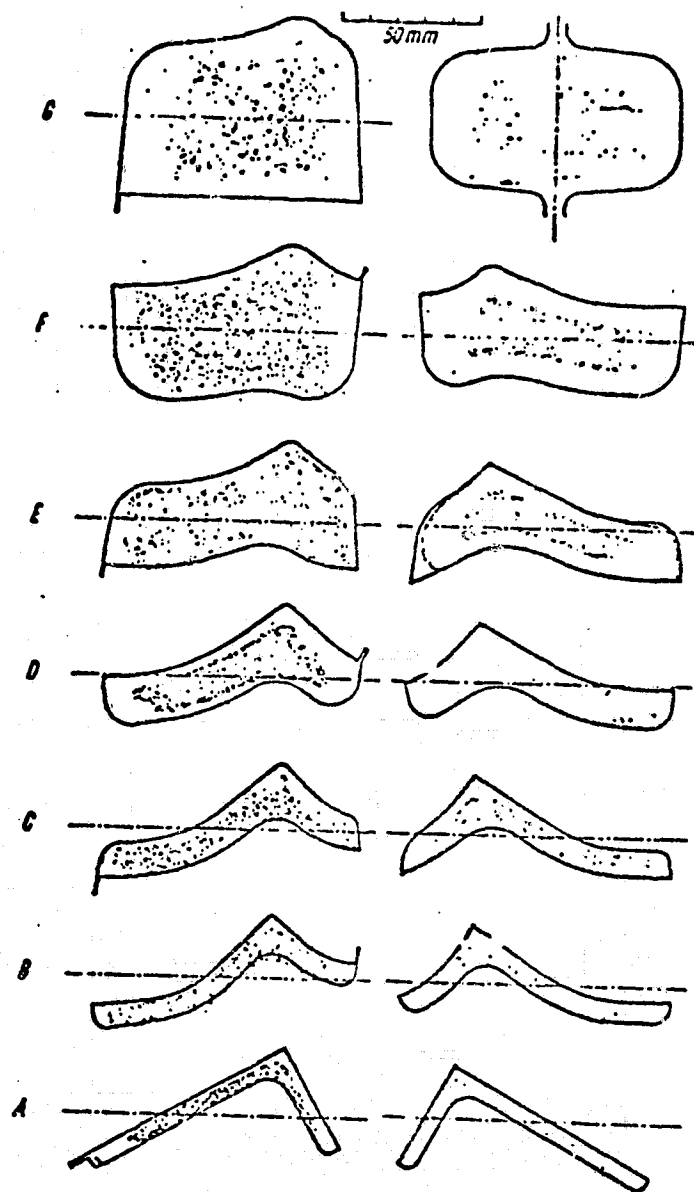


FIGURE 4. SCHEMATIC OF TWO DIFFERENT ROLL-PASS DESIGNS FOR A STEEL ANGLE WITH UNEQUAL LEGS (7)

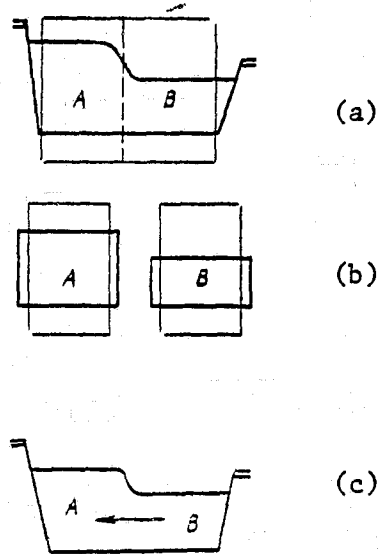


FIGURE 5. NONUNIFORM DEFORMATION IN ROLLING OF A SHAPE

(c) the wear of the rolls must be minimized. The maximum value of the reduction per pass is limited by (a) the excessive lateral metal flow which results in edge cracking, (b) the power and load capacity of the roll stand, (c) the requirement for the rolls to bite in the incoming bar, (d) roll wear, and (e) tolerance requirements.

DETERMINATION OF FLOW STRESS, WORKABILITY AND FRICTION FACTOR

The two basic material characteristics that greatly influence the rolling process are the flow stress and the workability of the material being rolled. The flow stress represents the resistance of a material to plastic deformation, and the workability represents its ability to deform without failure, regardless of the magnitude of the local stress and strain rate required for deformation. In rolling of airfoil shapes, relatively moderate strains and strain rates are encountered in the deforming material. Consequently, the response of the alloys of interest must be determined in the practical range of temperatures, strains, and strain rates. Another important variable to be characterized is the friction factor (ratio of frictional shear stress to shear flow stress) at the tool-material interface.

Flow Stress and Its Determination. For a given metal, the flow stress is most commonly obtained by conducting the uniform compression tests without barreling⁽¹⁰⁾. In this test, a well-lubricated, short cylindrical specimen, machined from the material under study, is compressed between a pair of hardened flat parallel platens. At hot-working temperatures, the test is conducted in a fixture, as shown in Figure 6. The flow stress of a material is influenced by the conditions of the deformation process, mainly the temperature of deformation (θ), the degree of deformation or the strain ($\bar{\epsilon}$) and the rate of deformation or the strain rate ($\dot{\bar{\epsilon}}$). Therefore, the uniform compression tests must be conducted at the temperature and the strain-rate conditions that exist in the practical deformation process, under consideration. The degree of deformation, or the strain, is generally defined in terms of logarithmic (true) strain $\bar{\epsilon}$. In uniform upset test, the strain $\bar{\epsilon}$ is given as below:

$$\bar{\epsilon} = \ln \left[\frac{h_0}{h} \right], \quad (1)$$

where h_0 = initial sample height
 h = instantaneous sample height

The strain rate $\dot{\epsilon}$ is the derivation of strain $\bar{\epsilon}$ with respect to time or:

$$\dot{\epsilon} = \frac{d\bar{\epsilon}}{dt} = \frac{dh}{hdt} = \frac{V}{h}, \quad (2)$$

where V = instantaneous compression speed

In all metalworking operations, except in uniform compression, $\bar{\epsilon}$ and $\dot{\epsilon}$ values vary within the deforming material. Consequently, in using strains and strain rates in practical rolling operations, average values must be employed.

Workability and Its Determination. Workability of a metal represents its ability to deform without failure, regardless of the magnitude of the local stress and strain rate required for deformation. The nonuniform compression test and the torsion test are two of the most commonly used methods for evaluating workability of metals and alloys⁽¹¹⁾. Although there is no general agreement as to which test gives the best result, it was decided to measure workability using the nonuniform compression test, since the stresses in compression of cylinders and rolling of shapes are primarily compressive in nature. In these tests, a cylindrical specimen is compressed under two flat platens without any lubrication. The workability of the material is measured in terms of percent reduction in height to visible fracture on the specimen surface.

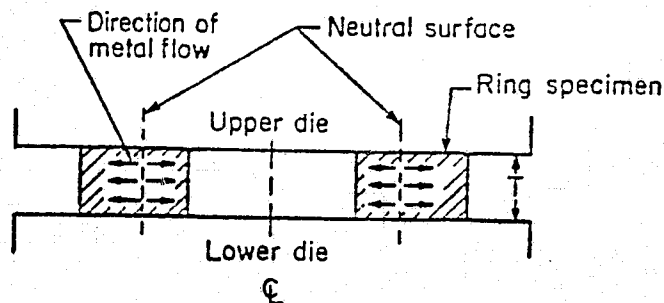


FIGURE 6. METAL FLOW IN RING COMPRESSION TEST

Friction Factor and Its Determination with the Ring Test. Friction at the tool-workpiece interface is another important process variable which needs characterization in order to be used in making predictions from analytical models. For this purpose, the friction factor associated with the actual rolling conditions is determined by using the well-established Ring Test⁽¹²⁾. The ring test consists of compressing a flat ring-shaped specimen to a known reduction, Figure 6. The change in internal and external diameters of the forged ring is very much dependent upon the friction at the tool-specimen interface. The internal diameter of the ring is reduced if the interface friction is large; increased if friction is low. Thus, the change in the internal diameter represents a simple method for evaluating interface friction.

In hot forming, as die temperatures usually are lower than billet temperatures, die chilling results. This effect influences the frictional conditions, and it is included in the measurement of the friction factor by using the ring test at hot-forging temperatures. Die chilling, however, also influences the temperature of the deforming billet and, consequently, its flow stress. It is, therefore, difficult to estimate the actual flow stress, $\bar{\sigma}$, and the friction factor, f , (or the shear factor, m) under practical rolling conditions. If these two values are known, shear stress, τ , is given by:

$$\tau = \bar{\sigma} \frac{m}{\sqrt{3}} = \bar{\sigma} f \quad . \quad (3)$$

To obtain the magnitude of the friction, the internal diameter of the compressed ring must be compared with the values predicted by using various friction factors, f , or shear factors, m . For this purpose, the upper-bound analysis and the associated computer program were developed earlier at Battelle and are available for use⁽¹²⁾. The computer program mathematically simulates the ring-compression process for given shear factors, m , by including the bulging of the free surfaces. Thus, ring dimensions for various reductions in height and shear factors (m) can be determined. This is the conventional way of representing theoretical calibration curves used in evaluating friction with the ring test.

In determining the value of the shear factor (m) for a given experimental condition, the measured dimensions (reduction in height and variation in internal diameter) are placed on the appropriate calibration figure. From the position of that point with respect to theoretical curves given for various m 's, the value of the shear factor (m), which existed in the experiment, is obtained.

MATERIAL DEFORMATION STUDIES

Materials

As mentioned earlier, mild steel (AISI 1018) as model cold rolling material and Ti-6Al-4V alloy as typical hot-working material were selected. INCONEL 718 (INCO 718) was selected as a material currently being used in cold rolling of airfoil sections. The nominal composition of these materials is given in Table I.

All the materials were ordered in round bar stock. The mild steel bars were cold drawn, the Ti-6Al-4V and INCO 718 bars were hot finished, rough ground and solution treated. The specimens for uniform compression tests were machined from 12.7 mm diameter bar stock, whereas the ring specimens were machined from 19.05 mm diameter bar stock. All the specimens were cut in the longitudinal direction, annealed at appropriate temperatures and shot blasted prior to testing (except Ti-6Al-4V).

Flow Stress

In the present work, specimens were machined to a nominal diameter of 12.7 mm (0.500 inch), a nominal height of 19.1 mm (0.750 inch), and sharp corners were broken. Mild steel and INCO 718 specimens were cleaned with acetone and placed on teflon sheets in between hardened steel platens (65 Rockwell C). The test conditions are summarized in Table II.

The AISI 1015 tests were conducted in a Baldwin universal testing machine of 267 kN (60,000 lb) capacity. More load was required for INCO 718; hence, a 445 kN (100,000 lb) capacity machine was used. The teflon sheets were replaced at every 10% reduction in order to ensure adequate lubrication and prevent bulging. Three specimens of each material were tested and the load-displacement curve was recorded.

TABLE I. NOMINAL COMPOSITION OF THE ALLOYS USED IN THE PRESENT PROGRAM

<u>AISI 1018 Steel</u>			
C	0.15 - 0.20	Mn	0.60 - 0.90
P,max	0.040	S,max	0.050
Fe	Balance		
<u>Ti-6Al-4V Alloy</u>			
Al	5.5 - 6.75	V	3.5 - 4.5
Fe	0.30	O	0.20
C	0.10	N	0.05
H	0.0125	Ti	Balance
<u>INCONEL 718 Alloy*</u>			
Cr	18.28	Fe	17.70
Al	0.65	Ti	1.03
Mo	3.07	Cu	0.17
Cb + Ta	5.15	C	0.04
Mn	0.15	Si	0.17
Cu	0.04	S	0.003
P	0.013	B	0.002
Ni	Balance (53.43)		

* As supplied by the vendor.

TABLE II. UNIFORM COMPRESSION TEST CONDITIONS

MATERIAL	CONDITION	TEST TEMP.	TEST MACHINE	CROSSHEAD SP.	LUBRICANT
AISI 1015	Annealed at 1600 F for 1 hr Furnace Cooled	Room Temperature	Baldwin Capacity 60.000 (1b)	0.02 inch/min	Teflon Sheet 0.010 inch
INCO 718	Annealed at 1800 F for 1 hr Air Cooled	Room Temperature	Baldwin Capacity 100.000 (1b)	0.02 inch/min	Teflon Sheet 0.010 inch
TI-6Al-4V	As Received	1700 F	Baldwin Capacity 60.000 (1b)	1 inch/min	Window Glass

- NOTES: 1) Nominal dimensions of all samples were 0.500-inch diameter x 0.750-inch high.
 2) During the tests that were conducted at room temperature, the lubricant (teflon sheet) was renewed at every 10 percent reduction.

The Ti-6Al-4V tests were conducted under isothermal conditions at 927 C (1700 F) using powdered window glass as lubricant. Ti-6Al-4V was tested at 927 C as it is a typical hot-working temperature for this alloy. The experimental fixturing is illustrated in Figure 7. A spiral groove was machined at the ends of each specimen to enhance lubricant retainment and ensure uniform upset conditions. Three specimens were tested and the load-displacement curve was recorded. From the load-displacement curves, the necessary calculations to obtain the flow stress versus strain curves, given in Figures 8 through 10 were made using a simple computer program.

The microstructure of Ti-6Al-4V compression test specimens was examined at the NASA-Lewis Research Center. Sections perpendicular to the applied stress (cross section) and parallel to the applied stress (longitudinal section) were mounted, polished, and etched (2 parts HCl, 1 part HF) for the as-received material and the six isothermally compressed specimens. In addition, a piece of as-received alloy, which was subjected to a heat treatment (placed in furnace at approximately 677 C (1250 F); slowly heated to 927 C (1700 F) over 2 hr; held for a few minutes at 927 C (1700 F); air cooled) designed to simulate the thermal portion of the compression test cycle was also examined.

The microstructure of as-received alloy is shown in Figure 11. The structure consists of large alpha grains surrounded by small beta and alpha grains. This microstructure is similar in appearance to that shown in Figure 2724 of the Metals Handbook, Vol. 7 (Reference 14) and is the result of a fabrication schedule involving work above the beta transus temperature followed by significant amounts of work in the two phase (alpha plus beta) temperature range. The microstructure of the heat-treated material is shown in Figure 12. It consists of primary alpha (large alpha grains present before heat treatment, see the longitudinal section of Figure 11), acicular alpha, and intergranular beta. This microstructure is similar to that shown in Figures 2713 and 2714 of the Metals Handbook, Vol. 7 (Reference 14). Comparison of Figures 11 and 12 indicates that heat treatment is tending to form an equiaxed microstructure about 10 μ m in diameter; however, definite signs (primary alpha) of the as-received microstructure remain.

In general, the microstructures of the tested samples (6 samples with true strain ranging from -0.37 to -0.71) are identical and consist of equiaxed alpha grains about 4 μ m in diameter and intergranular beta (very small distinct particles), as shown in Figure 13. The microstructure is somewhat similar to

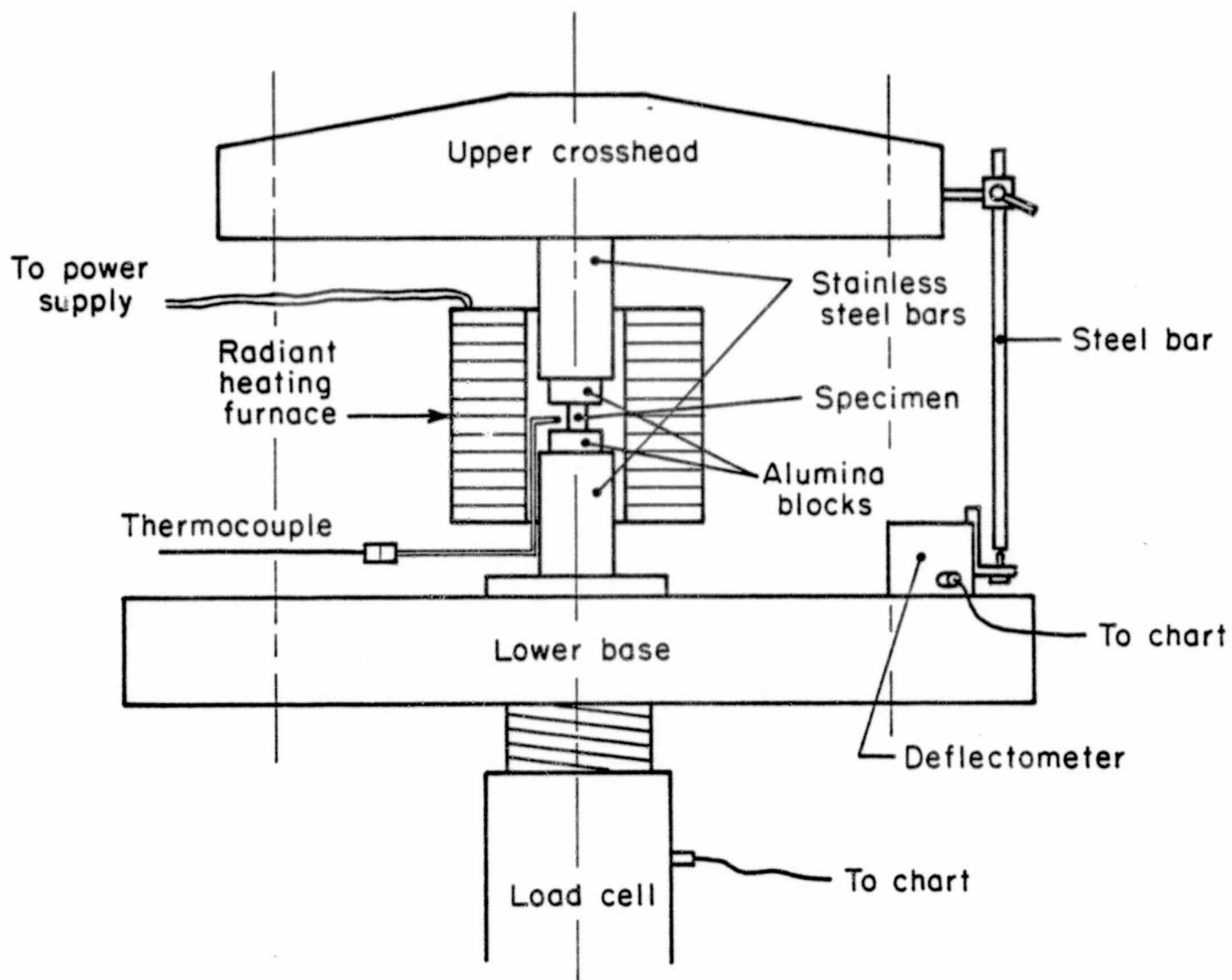


FIGURE 7. EXPERIMENTAL SET UP ON A UNIVERSAL TESTING MACHINE FOR HOT UPSET TESTS

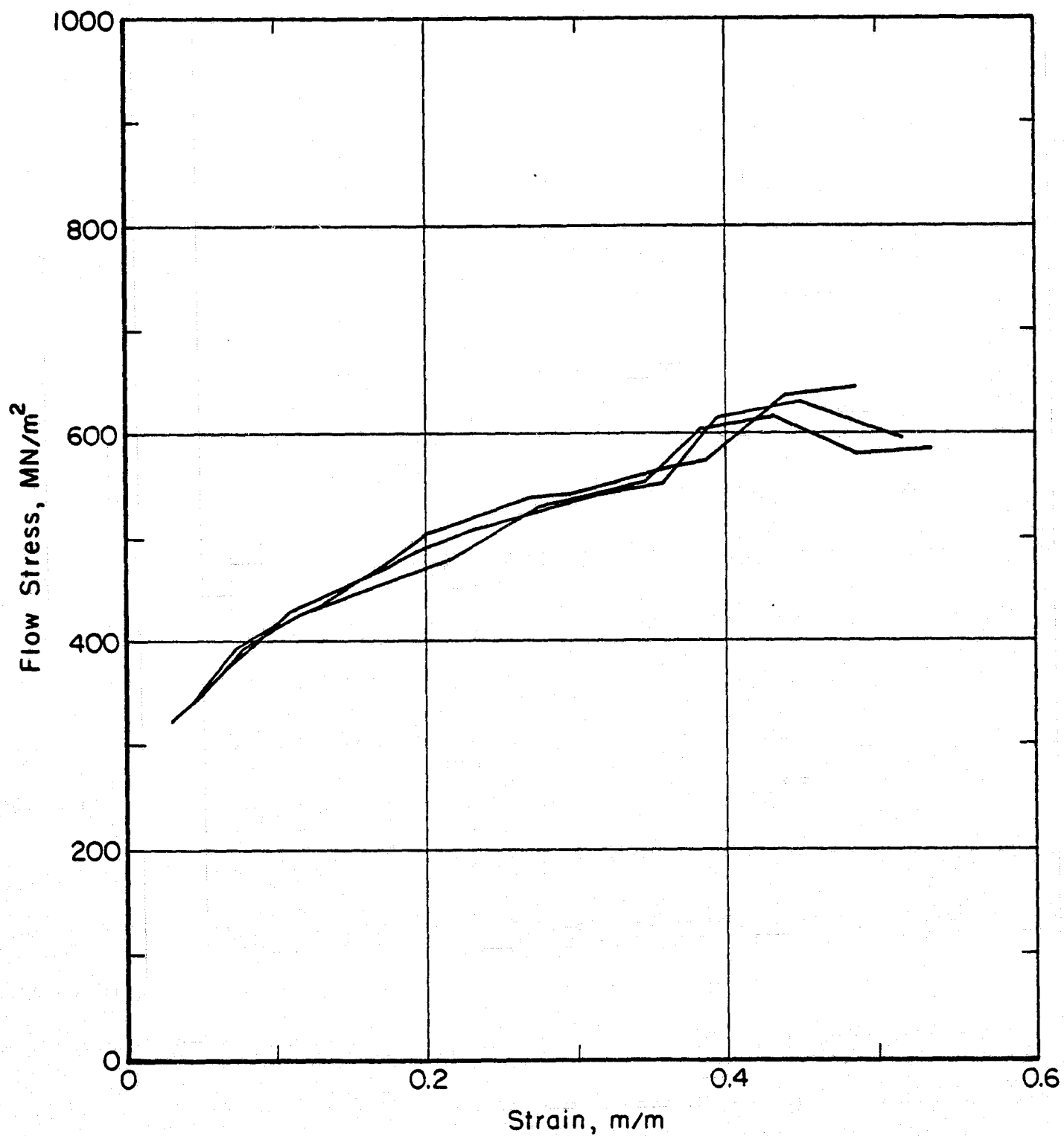


FIGURE 8. UNIFORM COMPRESSION TEST RESULTS FOR AISI 1015 AT ROOM TEMPERATURE

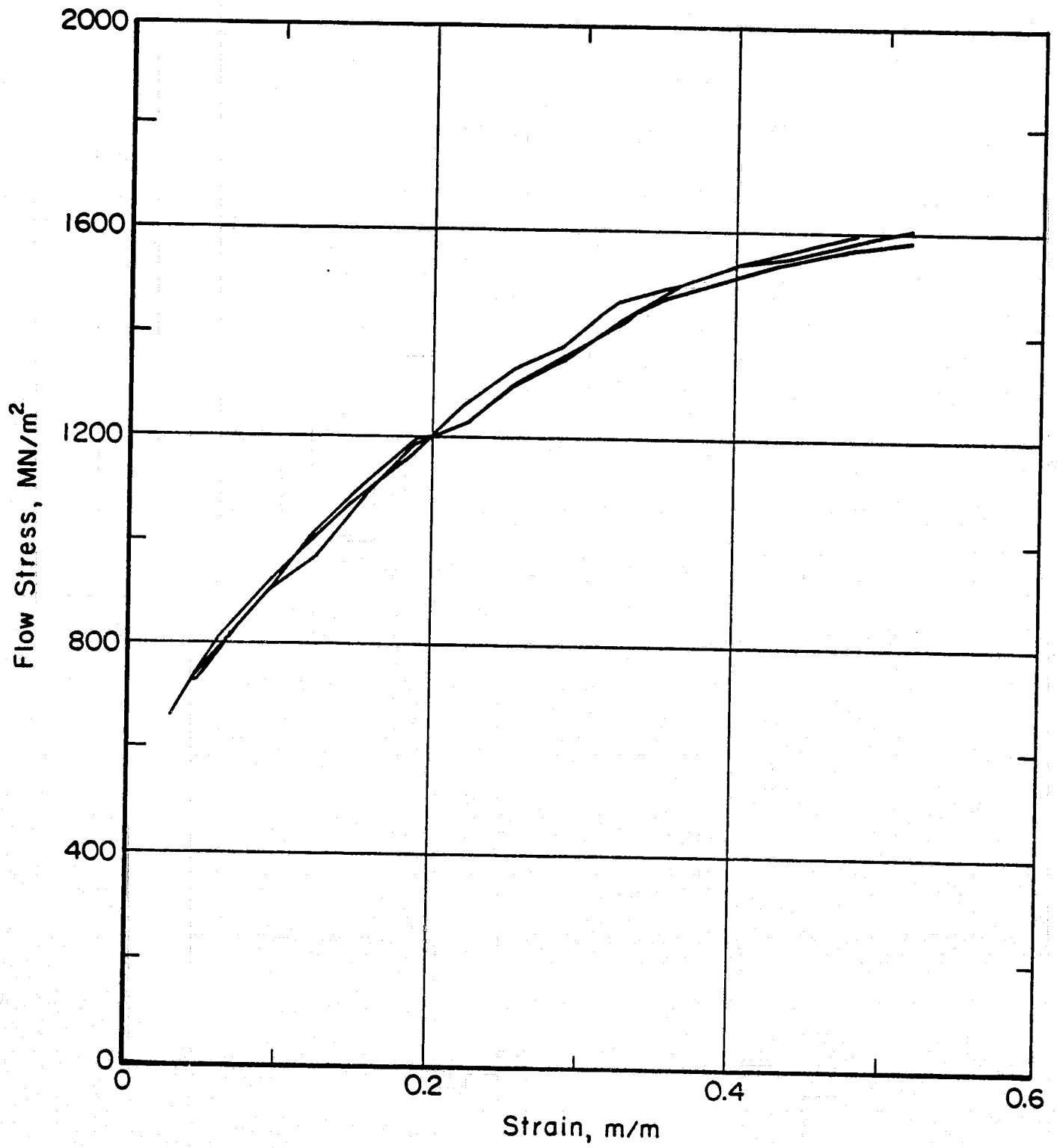


FIGURE 9. UNIFORM COMPRESSION TEST RESULTS FOR INCO 718 AT ROOM TEMPERATURE

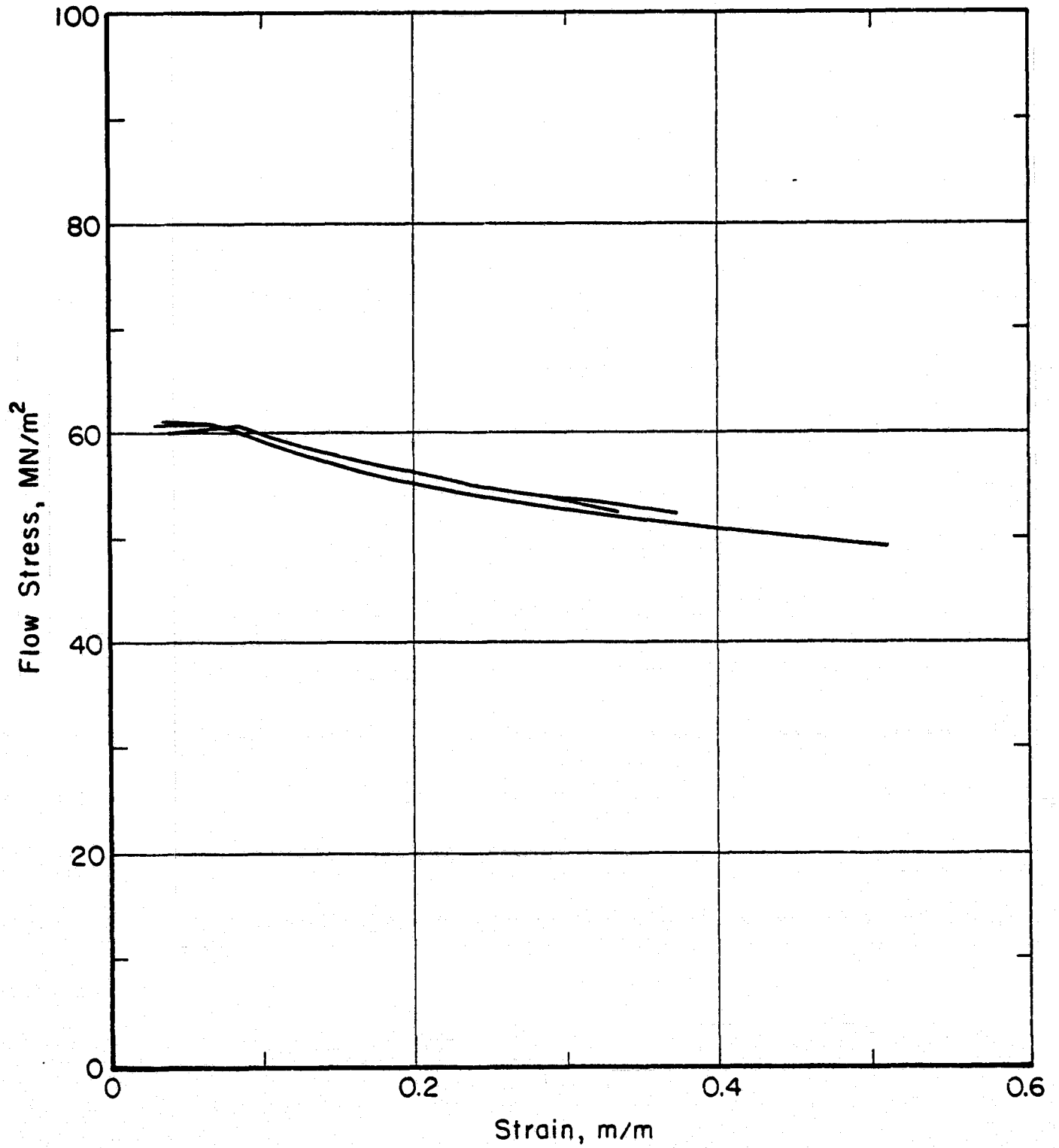
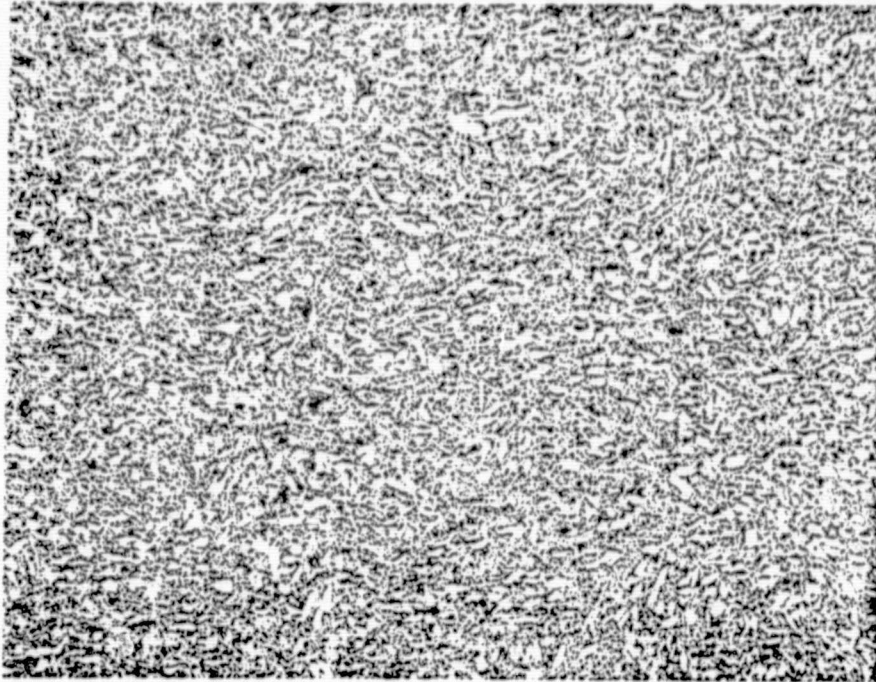
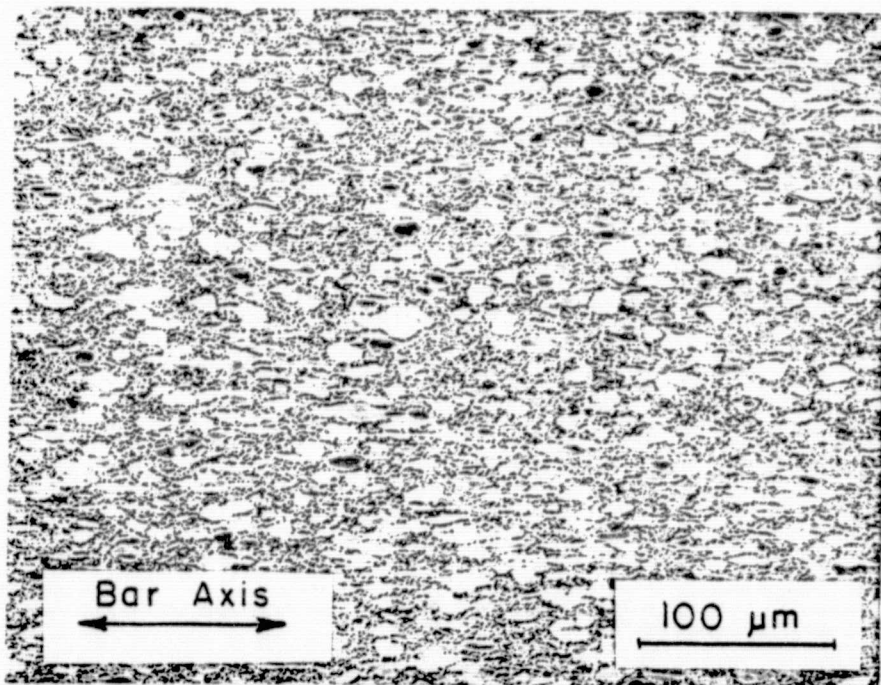


FIGURE 10. UNIFORM COMPRESSION TEST RESULTS FOR Ti-6Al-4V AT 927 C (1700 F)



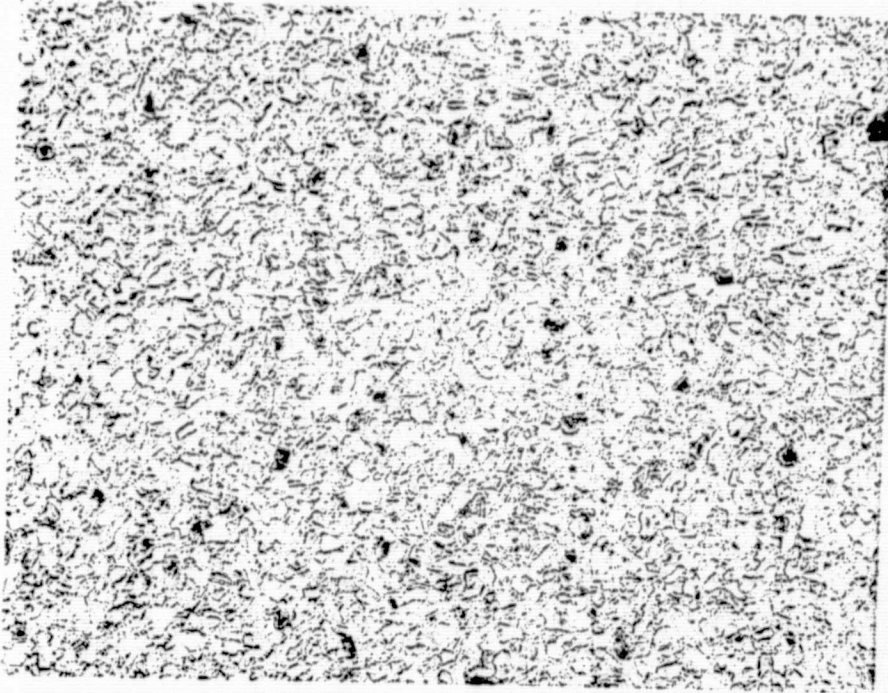
As-Received Cross Section



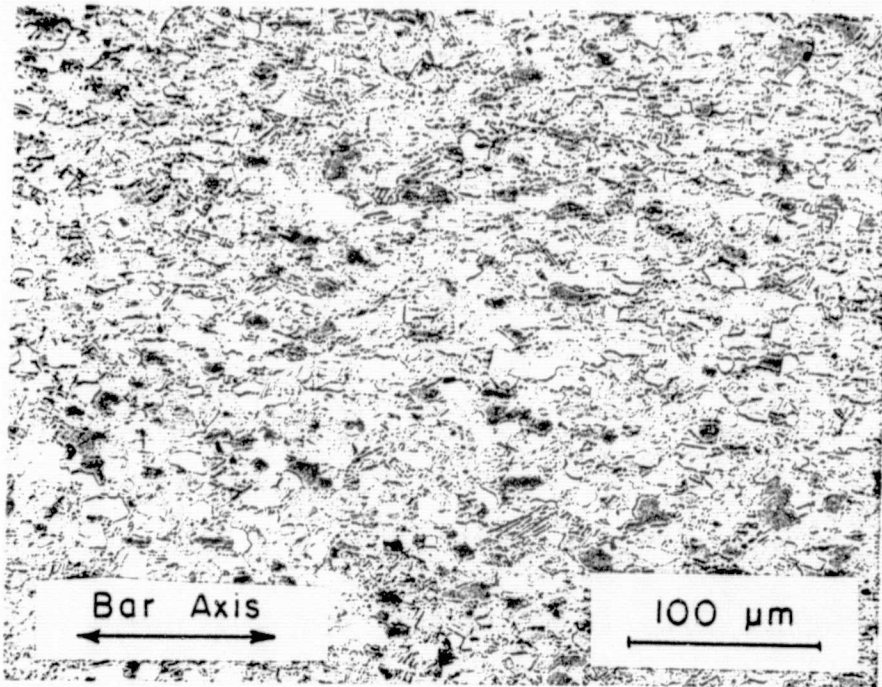
As-Received Longitudinal

FIGURE 11. PHOTOMICROGRAPHS OF AS-RECEIVED Ti-6Al-4V

ORIGINAL PAGE 19
OF POOR QUALITY



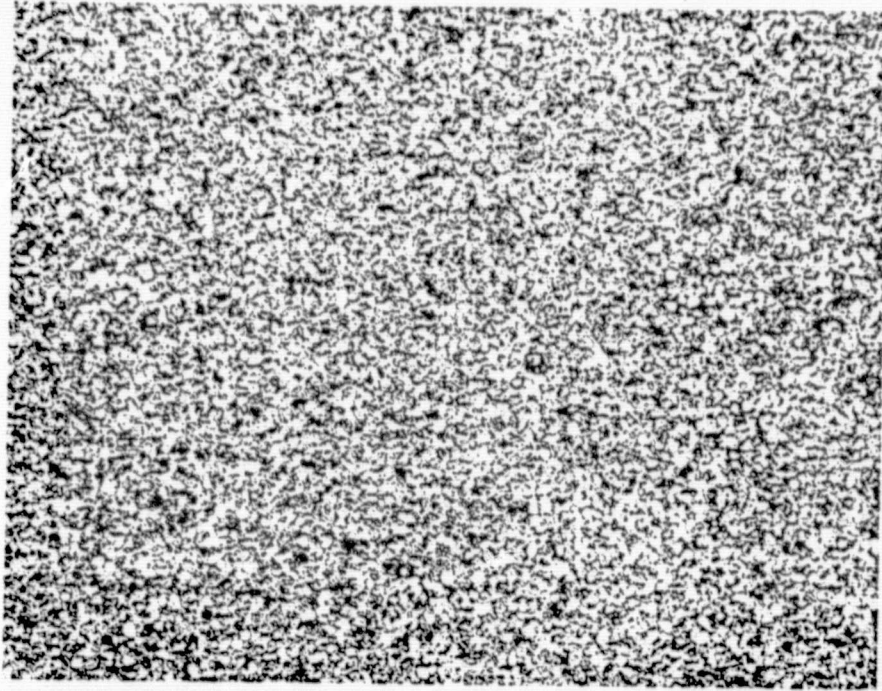
Heat Treated Cross Section



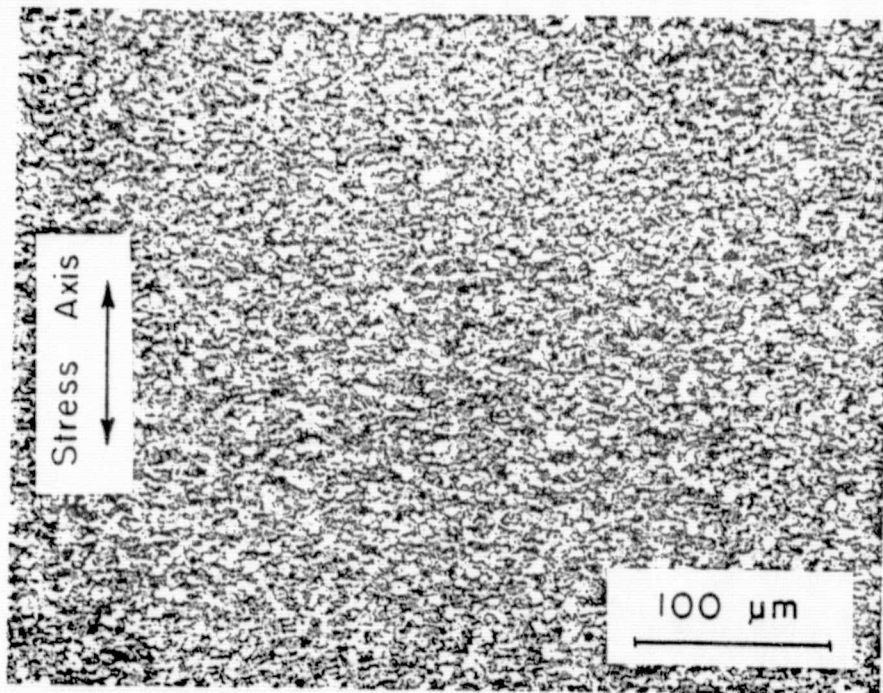
ORIGINAL PAGE IS
OF POOR QUALITY

Heat Treated Longitudinal

FIGURE 12. PHOTOMICROGRAPHS OF HEAT-TREATED Ti-6Al-4V



Specimen 1 Cross Section



Specimen 1 Longitudinal

FIGURE 13. PHOTOMICROGRAPHS OF TEST SPECIMEN AFTER COMPRESSION TEST
($\bar{\epsilon} = -0.56$, $t = .428$, $t_0 = 0.75$, $\epsilon = \ln t/t_0$)

those in Figures 2712 and 2719 of the Metals Handbook, Vol. 7 (Reference 14). Comparison of the microstructures of the tested specimens to the heat-treated specimen (Figure 12) indicates that working has fully developed a small equiaxed grain structure which is apparently not significantly affected by the work levels investigated in this study (true strains ranging from -0.37 to -0.71). Attempting to correlate the observed microstructure with mechanical behavior, it appears that some critical amount of work (approximately 10%, see Figure 9) must be introduced in order to start recrystallization. Once started, recrystallization is a dynamic process with the observed grain size remaining essentially constant over strain range investigated. This observation agrees with Luton and Sellars⁽¹⁵⁾ who indicated that the dynamic recrystallized grain size is function of the flow stress.

Workability

Workability tests were conducted for AISI 1015 and INCO 718 at room temperature. 12.7 mm (0.5-inch) diameter, 19.1 mm (0.750-inch) long nonlubricated cylindrical specimens were compressed in a universal testing machine until cracks appeared. AISI 1015 specimens were compressed 70 percent without any cracks, at which point the test was stopped. INCO 718 specimens showed classical 45 degree cracks at approximately 56 percent \pm 2 percent reduction consistently. Figure 14 shows an INCO 718 specimen which cracked at 56 percent reduction in height and an uncracked AISI 1015 steel specimen which was compressed to 70 percent reduction in height. Workability tests of Ti-6Al-4V have not been conducted as yet.

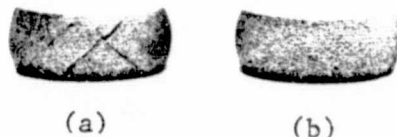


FIGURE 14. DEFORMED SAMPLES FROM NONUNIFORM COMPRESSION TESTS FOR DETERMINING WORKABILITY: (a) INCO 718 Specimen after 56 Percent Reduction, (b) AISI 1015 Steel Specimen after 70 Percent Reduction

Friction Factor

In the present work, ring tests with AISI 1015 and INCO 718 were conducted at room temperature using essentially the same experimental set up as that used for uniform compression and workability tests. Ring specimens were machined to have 19.1 mm (0.750-inch) OD x 9.52 mm (0.375-inch) ID x 6.35 mm (0.250-inch) height. Rings were upset between flat hardened platens to approximately 15, 30 and 40 percent reduction in height. In order to approximate the friction conditions, which are present during cold shape rolling in practice, the rings were dipped into a drawing lubricant (Turco Draw 300) prior to upsetting. After the tests, the dimensions of the rings were measured. The friction shear factor m was determined from the variation of the internal ring diameter by using the theoretical calibration curves given in Figure 15. The results show that the friction factor m is approximately 0.3 for INCO 718 and 0.25 for AISI 1015. Figure 16 shows AISI 1015 steel rings before deformation and after 20, 30 and 40 percent reduction in height.

The ring tests for Ti-6Al-4V, which must simulate the actual conditions of isothermal rolling, were postponed. These will be conducted at a later date after the conditions of the isothermal rolling tests are established.

ANALYSIS AND PREDICTION OF METAL FLOW

In rolling of shapes, the material elongates in the rolling direction as well as it spreads in the transverse direction. Thus, an analysis of deformation in rolling of airfoil shapes includes not only the determination of roll torque and the location of the neutral plane, but also the determination of spread in the transverse direction. The purpose of the present analysis is to determine the distribution of metal flow during rolling of a bar with an initial arbitrary section through a pair of rolls with airfoil-like contours. Based on this analysis, a computer program named SHPROL was coded to simulate the metal flow in rolling of airfoil shapes.

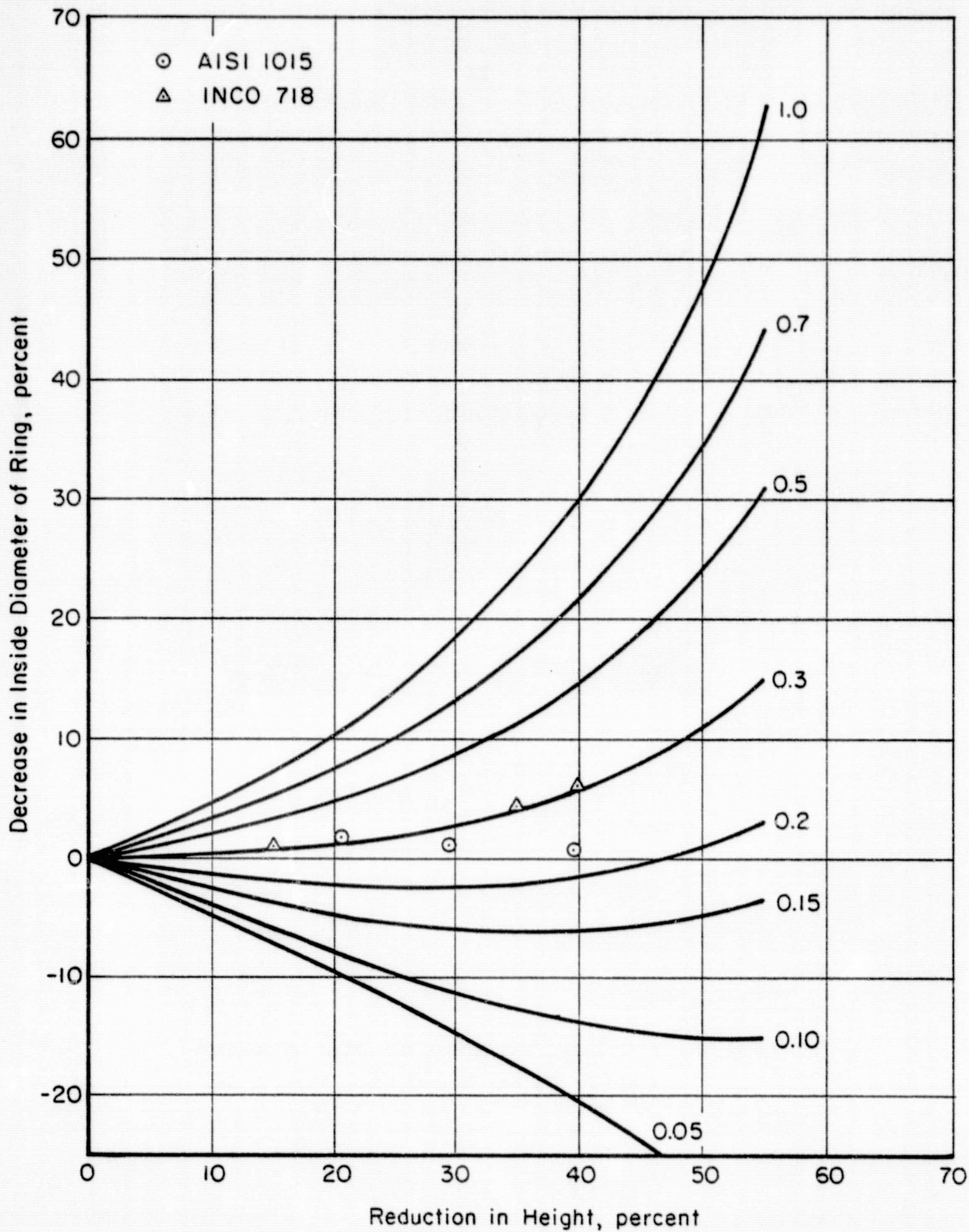


FIGURE 15. THEORETICAL CALIBRATION CURVES AND EXPERIMENTAL POINTS FOR DETERMINING FRICTION FROM UPSETTING 6:3:2 RINGS



FIGURE 16. AISI 1015 RINGS BEFORE AND AFTER DEFORMATION
(Left to Right: Reduction in Height 0, 20,
30 and 40 Percent, Respectively)

The present analysis employs the upper-bound type theory to predict the distribution of metal within the deformation zone between the rolls. One essential feature of applying the upper-bound technique to the present uncontained steady-state metal flow problem is to find a kinematically admissible velocity field which does not change the volume shape, and satisfies the volume constancy and the velocity boundary conditions. It is usually very difficult to find an admissible velocity field for problems involving general configurations even under nonsteady-state conditions. The condition of steady-state makes the problem of determining an admissible velocity field even more difficult. Therefore, a modular approach, somewhat similar to the finite-element method, is developed here and the following simplifying assumptions are made in performing the present analysis:

- (1) An airfoil shape can be considered as an aggregate of slabs, as shown in Figure 17.
- (2) Plane sections perpendicular to the rolling direction remain plane during rolling. Thus, the axial velocity (i.e., velocity in rolling x-direction) at any section perpendicular to the rolling direction is uniform over the cross section.
- (3) The velocity components in the transverse y, and the thickness z directions are functions of x and linear in y and z coordinates, respectively (see Figure 17).

The above assumptions correspond approximately to actual metal flow conditions and have been shown to yield good predictions of metal flow in rolling of plates.

Approach. The method used in solving the present problem is somewhat similar to the finite-element method in the sense that the deformation zone is divided into quadrilateral elements on the x-y plane, as shown in Figure 17. The divisions in the transverse (y-) direction are made such that the velocities normal to the dividing lines are zero. Thus, these lines represent streamlines of metal flow. However, a finite number of velocity discontinuities occur across the planes perpendicular to x-y plane and passing through these streamlines. The divisions along the longitudinal (x) direction, lines T_i-T_i , are made arbitrarily. Similarly, a finite number of velocity discontinuities occur

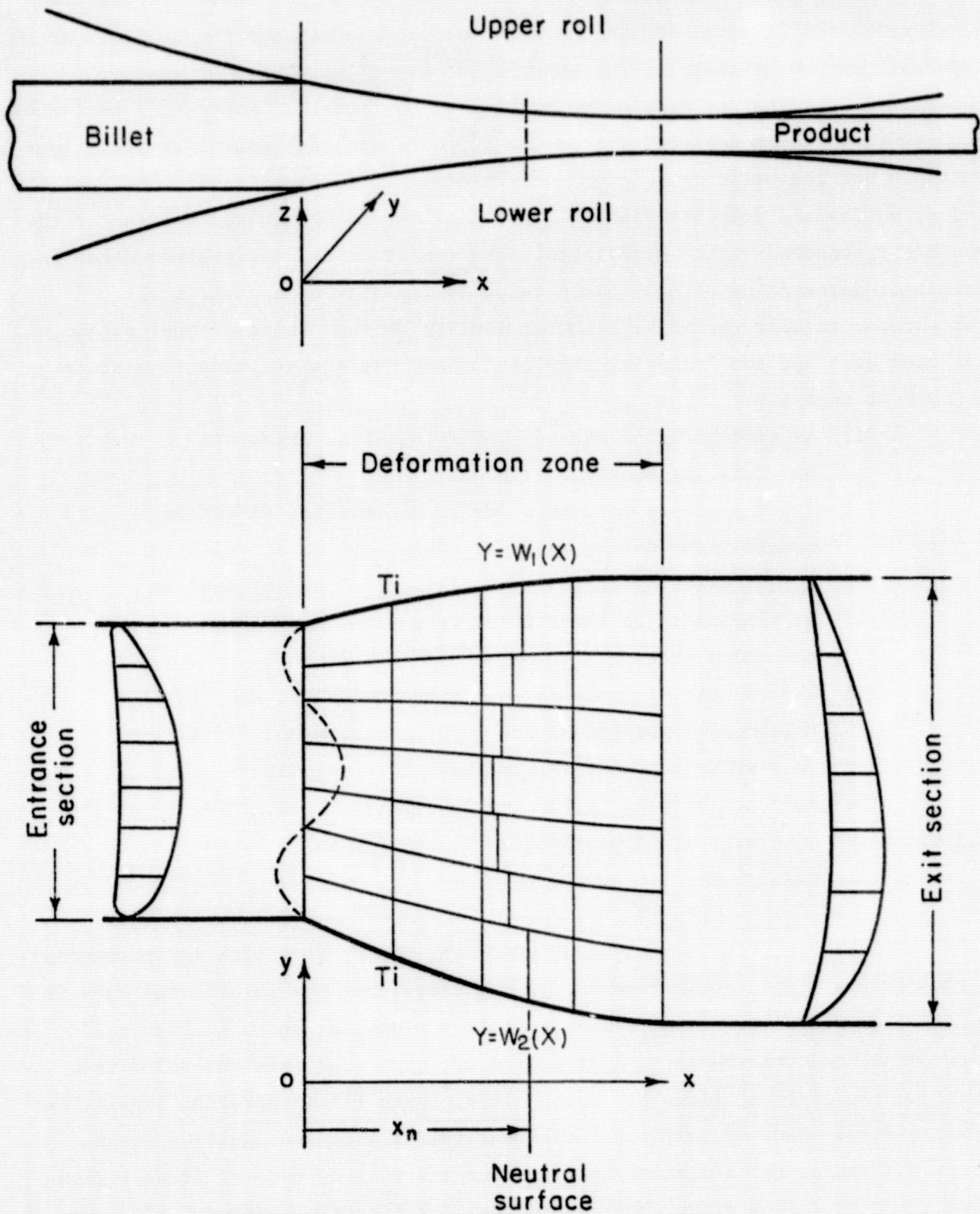


FIGURE 17. CONFIGURATION OF DEFORMATION ZONE IN ROLLING OF AIRFOIL SHAPES

across the y - z planes passing through these transverse lines, T_i-T_i , dividing the deformation zone.

It is assumed that the top and bottom surfaces of each element can be approximated by tapered planes, and the cross section of each element by a rectangle, as shown in Figure 18, where the area under a rectangle with broken lines is equal to the area of the original element. With this assumption, it is possible to treat each element as a plate for which it is possible to derive a kinematically admissible velocity field.

Velocity Field. The kinematically admissible velocity in the deformation zone for an element i is then given by:

$$\begin{aligned} V_x &= U v_x = U \frac{A_i(x_0)}{A_i(x)} \\ V_y &= U v_y = U v_x \frac{f'_1 (y - Y)}{f_1 - Y} \\ V_z &= U v_z = U v_x \frac{h'_1 (z - Z)}{h_1 - Z} \end{aligned} \quad (4)$$

where V_x , V_y , V_z are the velocity components in the x , y , z directions, respectively. U is the velocity of incoming strip and $A_i(x)$ is the area of cross section of the element at x . f , h , y and z are given in Figure 19 and the prime denotes a derivative with respect to x . In Figure 19 (ζ, ξ, η) is the local coordinate system of an element.

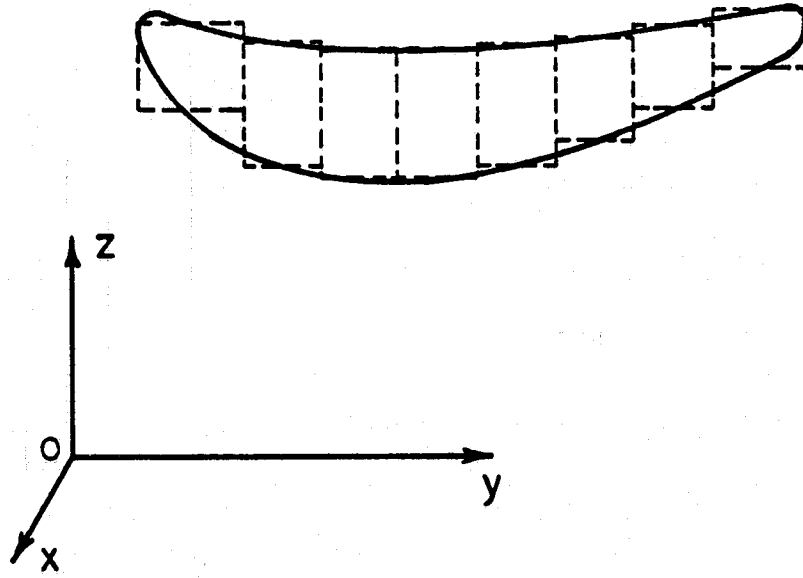


FIGURE 18. DIVISION OF AN AIRFOIL SECTION INTO RECTANGULAR ELEMENTS

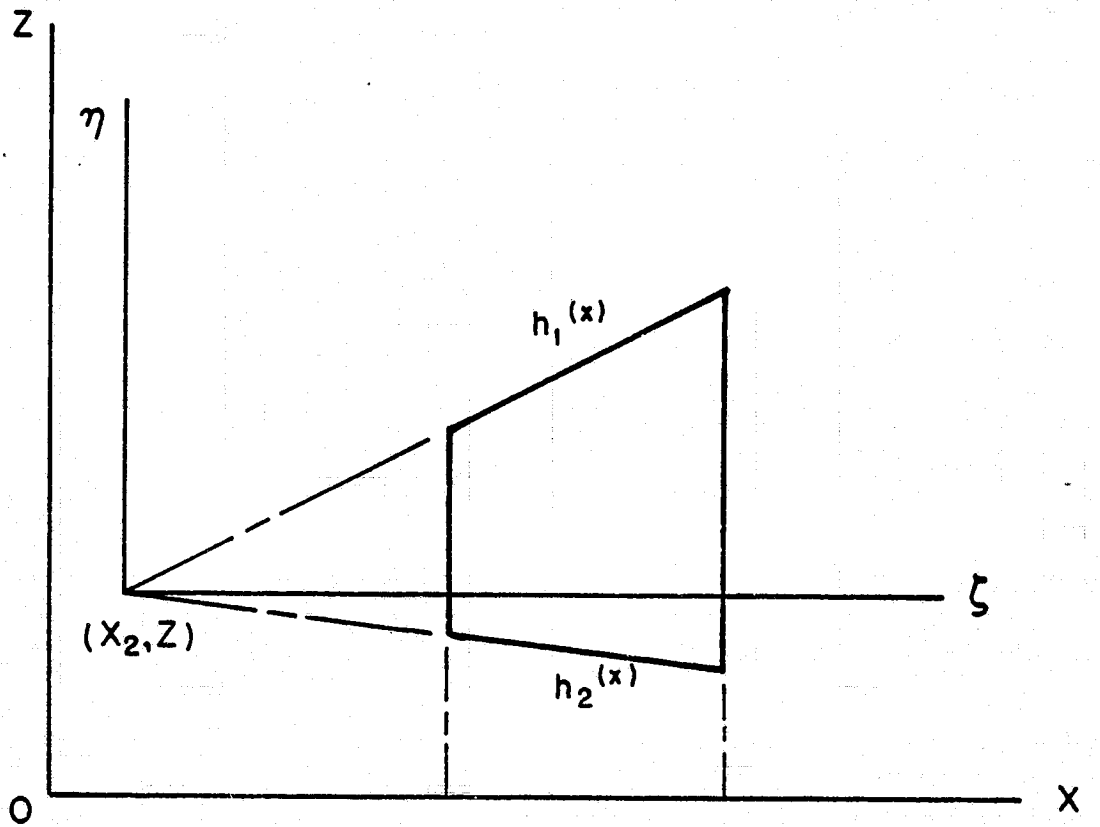
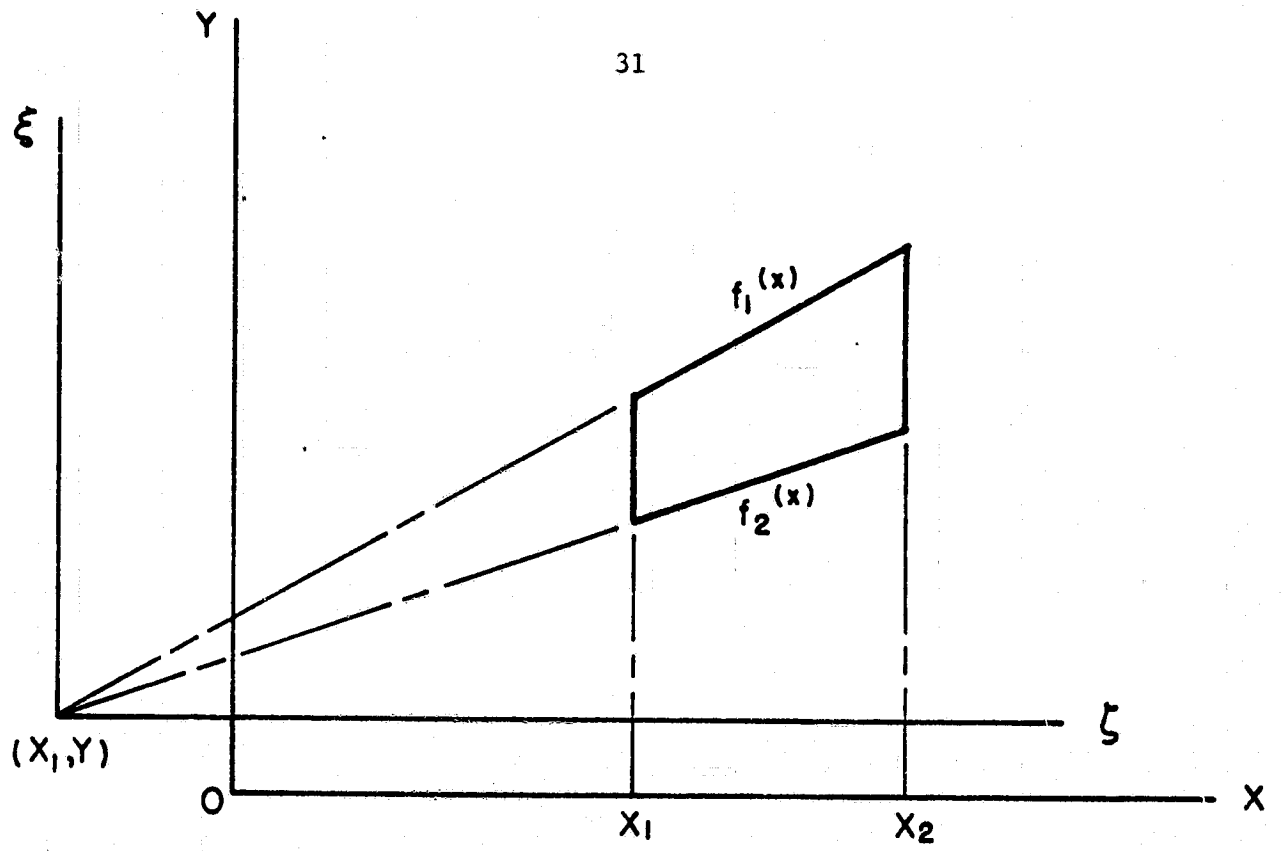


FIGURE 19. CONFIGURATION OF AN ELEMENT IN THE x - y AND x - z PLANES

The components of the strain-rate field can be derived from Equations (4). If $\dot{\epsilon}_x$, $\dot{\epsilon}_y$, and $\dot{\epsilon}_z$ represent the normal strain-rate components and $\dot{\gamma}_{xy}$ and $\dot{\gamma}_{xz}$ are the shear strain rates, then

$$\dot{\epsilon}_x = U \frac{\partial v_x}{\partial x}, \quad \dot{\epsilon}_y = U \frac{\partial v_y}{\partial y}, \quad \dot{\epsilon}_z = U \frac{\partial v_z}{\partial z}, \quad (5)$$

$$\dot{\gamma}_{xy} = U \left(\frac{\partial v_x}{\partial y} + \frac{\partial v_y}{\partial x} \right), \quad \text{and} \quad \dot{\gamma}_{xz} = U \left(\frac{\partial v_x}{\partial z} + \frac{\partial v_z}{\partial x} \right)$$

Total Energy Rate. The total energy rate of the process consists of the energy rate of plastic deformation, energy rate associated with velocity discontinuities and the energy rate to overcome the frictional restraint.

The energy rate of plastic deformation, \dot{E}_p , for an element is given as follows:

$$\dot{E}_p = \int_V \bar{\sigma} \dot{\epsilon} dV, \quad (6)$$

where $\bar{\sigma}$ is the flow stress of the deforming material, V is the volume of the element, and $\dot{\epsilon}$ is the effective strain rate given by:

$$\dot{\epsilon} = \frac{2}{3} \sqrt{\left(\dot{\epsilon}_x^2 + \dot{\epsilon}_y^2 + \dot{\epsilon}_z^2 + \frac{1}{2} \dot{\gamma}_{xy}^2 + \frac{1}{2} \dot{\gamma}_{xz}^2 \right)}$$

The energy rates associated with velocity discontinuities are due to shearing along the planes of velocity jumps. Across the transverse sections, velocity discontinuities can occur along the y - and the z - directions. Velocity discontinuities across the longitudinal sections can occur along the longitudinal direction and the z -direction. The energy rate due to velocity discontinuity along a section with area of cross section A is given as:

$$\dot{E}_d = \frac{\bar{\sigma}}{\sqrt{3}} \int_A |\Delta V| dA, \quad (7)$$

where ΔV is the velocity jump across the area A .

Energy is dissipated in overcoming the friction at the roll-workpiece interface. If ΔU is the velocity differential at the roll-workpiece interface with surface area S , the energy dissipation due to friction, \dot{E}_f , is given as below.

$$\dot{E}_f = \frac{m \bar{\sigma}}{\sqrt{3}} \int_S |\Delta U| dS \quad , \quad (8)$$

where m ($0 \leq m \leq 1$) is the friction shear factor at the interface.

The total energy dissipation rate, \dot{E} , is the sum of the deformation energy rate, the energy rates due to velocity discontinuities and the friction energy rate. The detailed derivations of each term will be included in the final report. \dot{E} is a function of unknown spread profiles w_1 and w_2 (see Figure 17) and the location of the neutral plane x_n . The unknown coefficients of w_1 and w_2 and x_n are determined by minimizing the total energy rate. The minimization of \dot{E} with respect to unknown parameters is done by numerical techniques. In order to keep the number of unknown variables to a minimum, the curves $y = w_1(x)$ and $y = w_2(x)$ are considered as a third order polynomials, each with two unknowns. The location of the neutral plane, $x = x_n$, is an additional unknown. Thus, a total of five independent variables, which are determined by minimization of the total energy rate, are sufficient for the formulation of the problem.

Computer Program. Based on the above modular upper-bound analysis, a system of computer programs, named SHPROL, was developed to predict metal flow in rolling of airfoil shapes. SHPROL is coded in FORTRAN IV and requires approximately 60,000 octal words of memory space in a CDC Cyber 70 computer. The properties of the material being deformed are provided through a subroutine named MATERL.

All the input data to the computer programs SHPROL are transferred through READ statements. This includes variables defining the number of elements in the deformation zone, shape and location of the preform section, shape and location of the upper and lower roll profiles, angular velocities of rolls, friction factor at the roll-workpiece interface, temperature of workpiece, and

some controlling variables for selecting proper options. A detailed description of these variables will be given in the input preparation. The flow stress of the deforming material, as a function of strain, strain rate and temperature, is furnished through a subroutine named MATERL, and it needs to be inserted in the program deck for the material under consideration.

The output from the program prints coordinates of the grid points, spread profiles as functions of axial distance (in rolling direction) from roll entry, the total energy dissipation rate and its various components, the location of the neutral plane, the extension rate as a function of axial distance, and the strain, strain rate and flow stress distribution in the deforming material. The output corresponds to a minimum total energy rate, which is minimized by a simplex method with respect to various unknown parameters. At the end of the execution, the output from the minimization routine is written on TAPE7. If further calculations are required, for example, to reduce the error of minimization, the contents of TAPE7 are read into TAPE8 and calculations are restarted from the point where they were left rather than from the beginning.

The computer program SHPROL was used to study the metal flow in finish rolling of GE's H-369 airfoil shape, which is used for stationary vanes in Stage 4 of the F-101 engine. The inlet strip shape was taken as the actual vane shape, except that its thickness was approximately 15 percent larger than the desired vane thickness. The rolling simulation was carried out using flow properties of mild steel, which was selected as a model material in the present investigation. Figure 20 schematically shows the results predicted by SHPROL. These values agree closely with the experimental observations in rolling of the same shape from INCO 718 at General Electric Company⁽¹⁶⁾.

The details of the computer program SHPROL will be included in the Final Report, together with instructions for preparing input to the program and a list of the important variable names used in the program SHPROL.

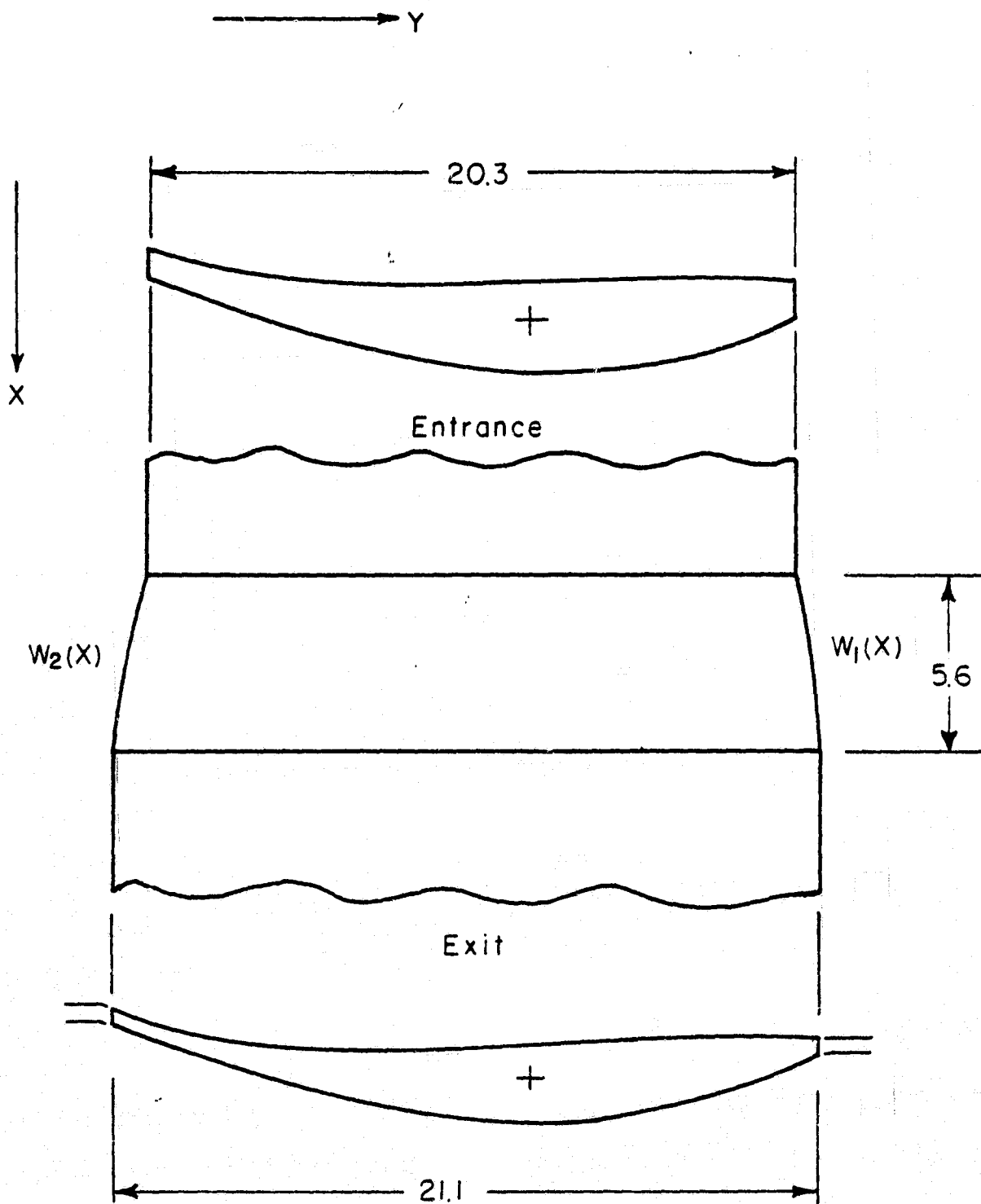


FIGURE 20. ROLLING OF GE'S H-369 AIRFOIL FROM MILD STEEL USING 203.2 mm ROLLS (AVG REDUCTION = 15.75 PERCENT, TORQUE = 1053 JOULES
 $w_1(x) = 0.4 + 0.027x - 0.061x^2$; $w_2(x) = -0.4 - 0.082x + 0.184x^2$)

MODELING FOR LOAD AND STRESS ANALYSIS

The objective of this effort is to derive a model for calculating the stress distribution on the rolls, the roll-separating forces and roll torque. The "Slab Method" was used in deriving the technique for load and stress analysis. The stress analysis, together with appropriate logic for handling geometry variation, was programmed for general use. The resulting computer program, ROLPAS, is capable of calculating the roll-separating forces, stress distribution and roll torque for most airfoil-like shapes. It can process rounds, slabs, diamonds, airfoils, but not T, H, U or other such shapes with a protrusion.

Description of Slab Method. The slab method, sometimes called "elementary theory" in European literature is an approximate method for analyzing plastic deformation problems and was originally applied by Siebel to various forming processes.

When applying the slab method, the following are usually assumed:

- (a) The material is isotropic and incompressible.
- (b) Elastic deflections are negligible.
- (c) Inertial forces are negligible.
- (d) Plane surfaces in the material remain plane.
- (e) Flow stress, $\bar{\sigma}$, is constant in the deformation zone studied.
- (f) The shear stress due to friction is expressed as $\tau = f\bar{\sigma}$, where f = friction factor.
- (g) Material flows according to von Mises' flow rule, i.e., for plane-strain deformation: $\sigma_z - \sigma_x = -\frac{2}{\sqrt{3}}\bar{\sigma}$;
for axisymmetric deformation: $\sigma_z - \sigma_r = -\bar{\sigma}$.

In light of the above assumptions, the equations for plane strain upsetting under inclined platens are derived for a deformation element using elementary stress analysis techniques.

The stress distribution is given by:

$$\sigma_z = \frac{K_2}{K_1} \ln \left(\frac{h_e}{h_b + K_1 x} \right) + \sigma_{ze}$$

where

$$K_1 = \tan \alpha + \tan \beta$$

$$K_2 = \frac{2K_1 \bar{\sigma}}{\sqrt{3}} + f \bar{\sigma} (2 + \tan^2 \alpha + \tan^2 \beta)$$

The notation is described in Figure 21.

Description of the Computer Program ROLPAS. The ROLPAS system was developed on a PDP-11/40 minicomputer using RT-11 operating system. In order to run ROLPAS with no (or minor) modifications, the following hardware and software components are required:

- (1) A PDP-11 series computer (except LSI-11) with a minimum of 28K words of memory operating under RT-11.
- (2) A random access external storage device such as a disk cartridge drive or a dual floppy disk drive.
- (3) A computer terminal (keyboard/printer) such as a teletype or DEC writer.
- (4) VT-11 display processor with a graphics CRT and light pen.
- (5) An x-y plotter interfaced to the PDP-11. Needed only if hard copies of the CRT graphics is desired.

ROLPAS was coded as an highly interactive program. Most man-machine interaction is achieved by use of the light pen and the extensive interactive capabilities of the display processor. When running ROLPAS, a menu of "operations" are displayed on the left side of the screen. Since ROLPAS is coded as a series of mathematical operations on the data base, this mode of interaction is a natural. At present, the following operations are defined:

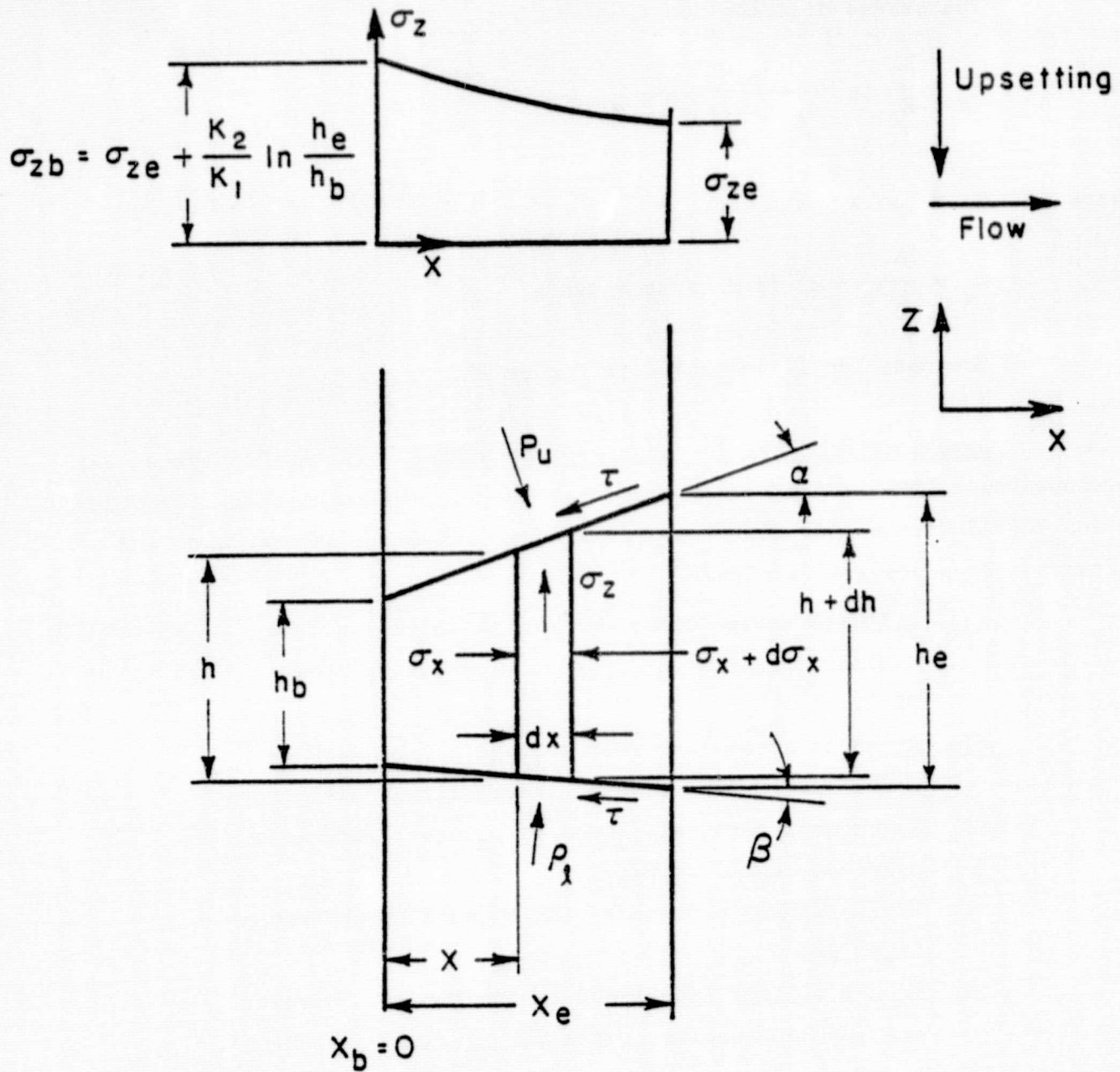


FIGURE 21. STRESSES IN PLANE-STRAIN UPSETTING BETWEEN INCLINED PLATES AND WITH UNIT DEPTHS (Divergent outward flow)

- Data Input: Read part geometry from data file.
- Check Input: Display the input geometry for visual checkout.
- Add Flash: Add flash to one or both sides of the input shape.
- Position Preform: Change the position of the preform with respect to the rolls. The user is allowed to move the preform anywhere on the screen with the light pen with respect to the rolls.
- Check Roll-Bite: Checks for roll-bite condition.
- Move the Rolls: Move the rolls up or down, thus opening or closing the exit cross section. Used for simulating different passes with the same rolls.
- Change Parameters: Can be called any time to change system parameters.
- Simulate Rolling: Simulates the rolling process, displaying each step as it steps from input to exit. The first step of the simulation of rolling an arbitrary preform through airfoil rolls is shown in Figure 22. Note that the input shape is preserved where it is not deforming. Figure 23 shows the last step of the simulation as the product exits from the rolls.
- Display Stress: Displays the stress distribution calculated during simulation. The display is a three-dimensional representation. Figure 24 shows the stress distribution obtained while rolling the preform of Figure 22. The shape of the contact zone and the spread pattern can also be ascertained from this display.
- Display Percent Elongation: Displays the distribution of elongation from entrance to exit along the exit cross section.
- Summarize Results: Provide an up-to-date summary of the results.

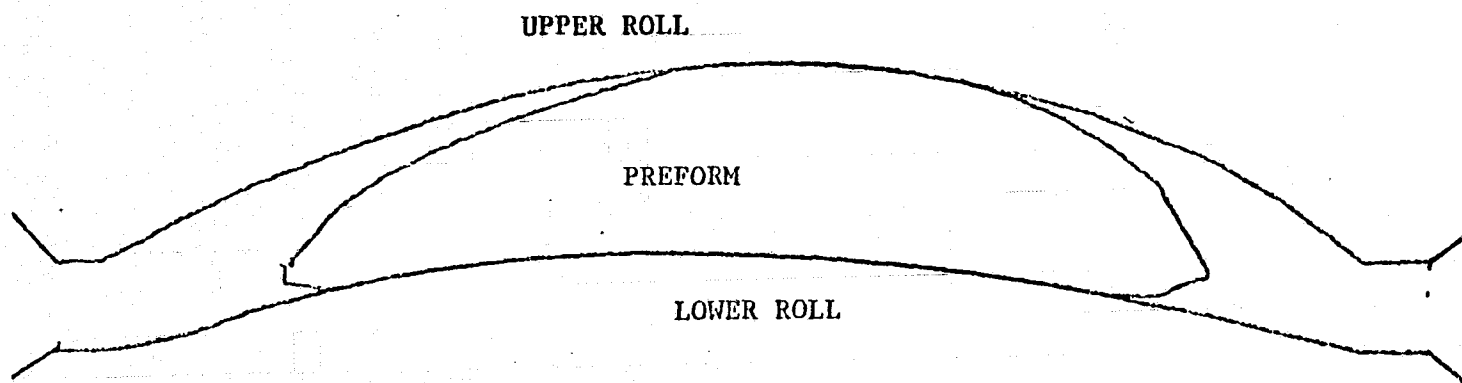


FIGURE 22. DEFORMATION OF A PREFORM AS IT ENTERS AIRFOIL SHAPED ROLLS.
THE STRESS OUTLINE IS LABELED AS STEP 1 IN FIGURE 24

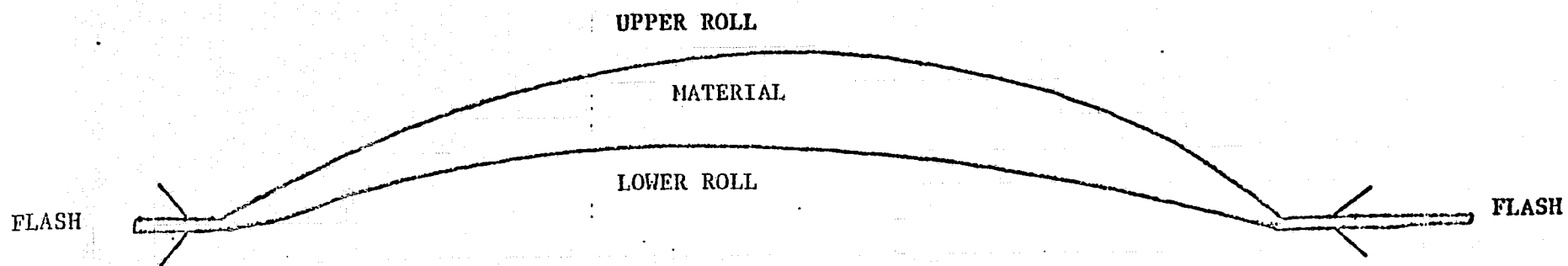


FIGURE 23. ROLLED AIRFOIL AS IT EXITS THE ROLLS. THE CALCULATED STRESS DISTRIBUTION IS DISPLAYED AT STEP 15 OF FIGURE 24

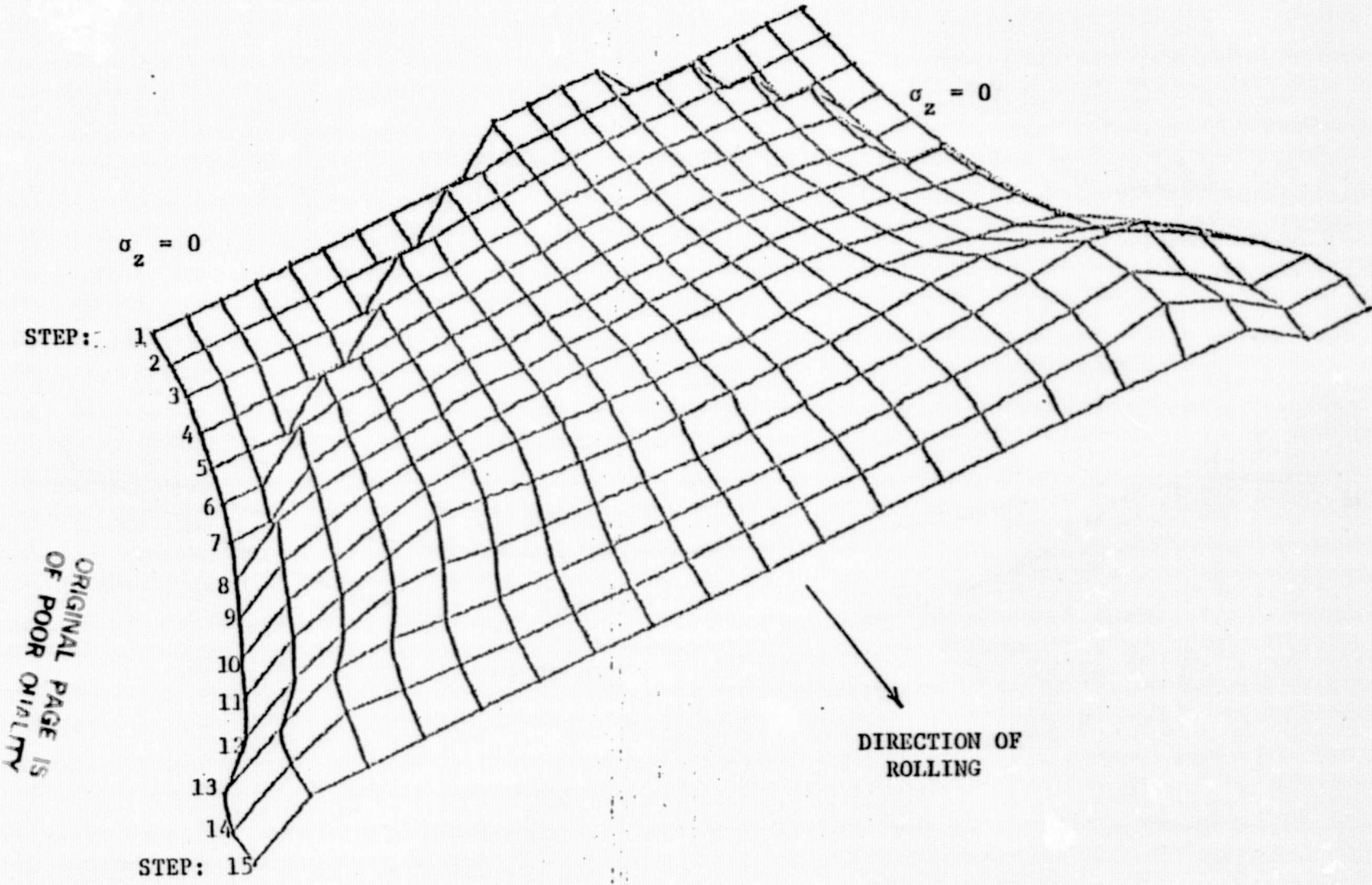


FIGURE 24. THREE DIMENSIONAL REPRESENTATION OF THE CALCULATED STRESS (σ_z) SURFACE FOR ROLLING OF THE SHAPE ILLUSTRATED IN FIGURE 22

At all times, only those operations that are logically allowable are displayed on the menu. This prevents execution of illogical sequences of operations by the user.

During simulation of rolling a shape, ROLPAS determines the geometry of the actual contact zone, a plan view of which is shown in Figure 25. Simulation starts at the entrance to the rolls and proceeds to the exit. At each step, one cross section parallel to the zx plane is processed. The geometry of the material at $j-1$ 'st section is input to the j 'th roll section. Stress distribution is calculated and the material is deformed according to the stresses and the elongation criteria. At the completion of simulation from entrance to exit, a stress analysis is performed along the streamlines of Figure 21. At each node of the mesh, the lower of the two σ_2 values is accepted as the actual stress. The stress surface is integrated to obtain the roll-separating force and the roll torque.

ROLPAS is intended to be a tool for use in the design of roll passes. To this end, the user, at his option, can simulate various designs and observe the shape produced. He can try different roll separations for the same preform. Using the percent elongation and percent reduction displays, he can make design decisions on how to modify his preform.

As discussed in the following sections, the results from ROLPAS have compared favorably with experimental observations on rolling of slabs.

EXPERIMENTAL EVALUATION OF COMPUTER MODELS

Experimental evaluation of the model for metal flow analysis and the model for load and stress analysis is being carried out in two phases. Under the first phase, it was planned to evaluate these models by using the existing experimental data on rolling of plates. However, the available experimental data on plate rolling are not described adequately in the literature, and were found insufficient for a complete evaluation of the models developed under this project. Therefore, a set of plate-rolling trials, both cold and hot, under controlled conditions, were undertaken. Under the second phase, it was planned to experimentally evaluate the validity of the computerized models of shape

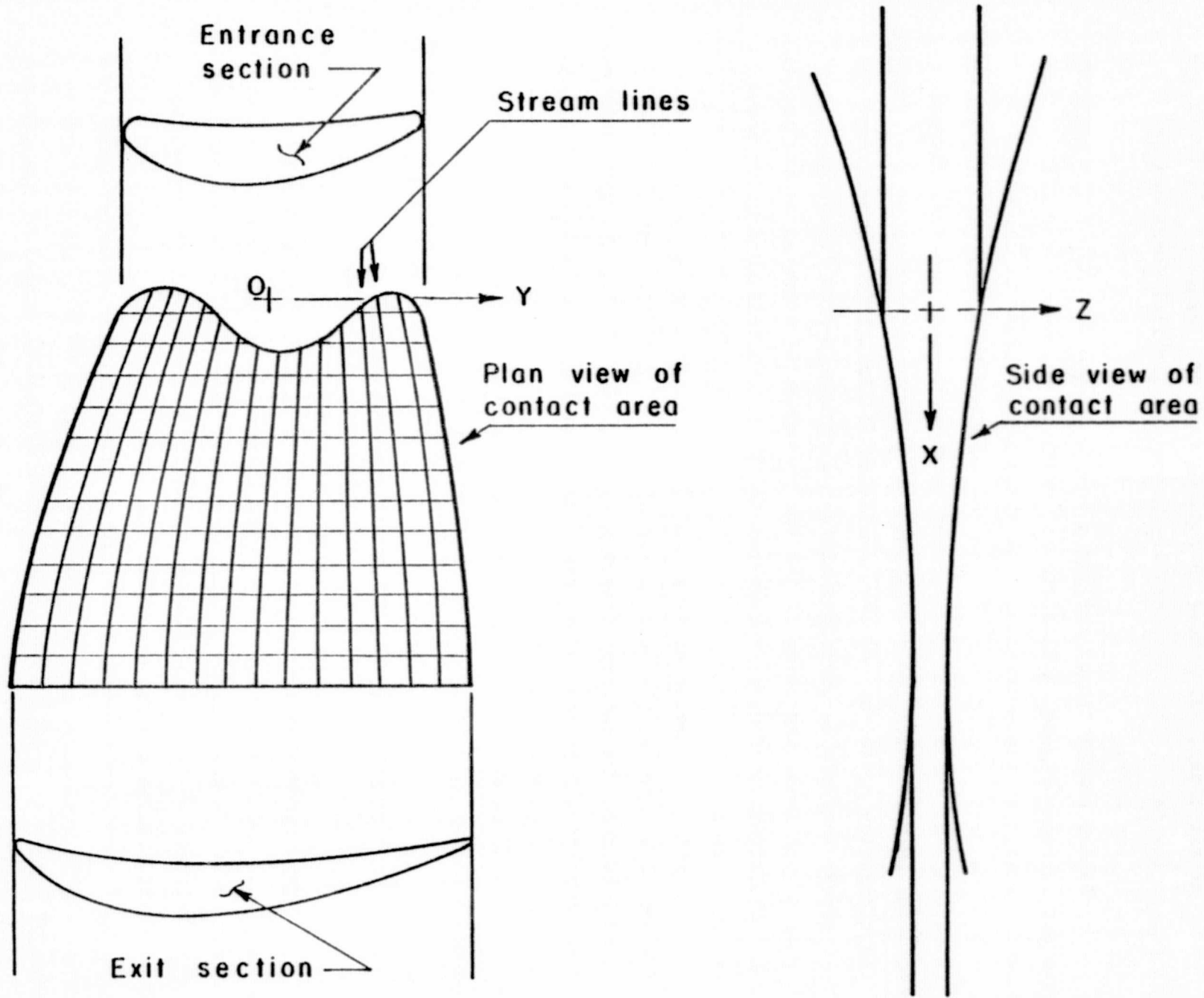


FIGURE 25. PLAN AND SIDE VIEWS OF THEORETICAL CONTACT AREA OF ROLLS AND MATERIAL DURING ROLLING OF AIRFOILS

rolling and roll-pass design by conducting laboratory experiments to roll an airfoil shape at room temperature from mild steel and under hot-isothermal conditions from Ti-6Al-4V alloy. In addition, it was planned to evaluate the computerized models with at least one commercial airfoil (or a similar shape) rolling process that is currently in production.

Plate-Rolling Experiments

One-inch thick mild steel (AISI 1018) steel plates were selected in widths of 1, 2, 3 and 4 inches, in order to have width-to-thickness ratios of 1, 2, 3 and 4, respectively. Nine-inch long rolling specimens were cut from each size, and were annealed, shot blasted and cleaned. Half of each size of specimens were cold rolled and the other half were hot rolled at 1000 C on an instrumented two-high rolling mill with 16-inch diameter x 24-inch long rolls. Specimens for hot rolling were heated in an electric furnace. No lubricant was used under both cold and hot-rolling conditions. The cold specimens were rolled up to a maximum of 25 percent reduction in height, in a single pass, in steps of 5 percent reduction in height. The hot specimens were rolled to a maximum of 50 percent reduction in height in a single pass, in steps of 10 percent reduction in height. During each rolling trial, the roll-separating force and the roll rpm were recorded on a brush recorder. The current (in ampere) and the voltage (in volt) across the mill motor were also recorded under idle and load conditions on a separate brush recorder. This information, together with roll rpm, was needed to approximately estimate the roll torque. The average height and width of each specimen before and after rolling were recorded.

Predictions of the roll-separating force and roll torque for cold rolling of plates were made by using the computer program ROLPAS. The friction and flow stress data for mild steel were taken from Task I results of this program. Theoretically predicted values of roll-separating force and roll torque, together with the experimental results, are shown in Figures 26 and 27. The agreement between theory and experiment appears to be very good.

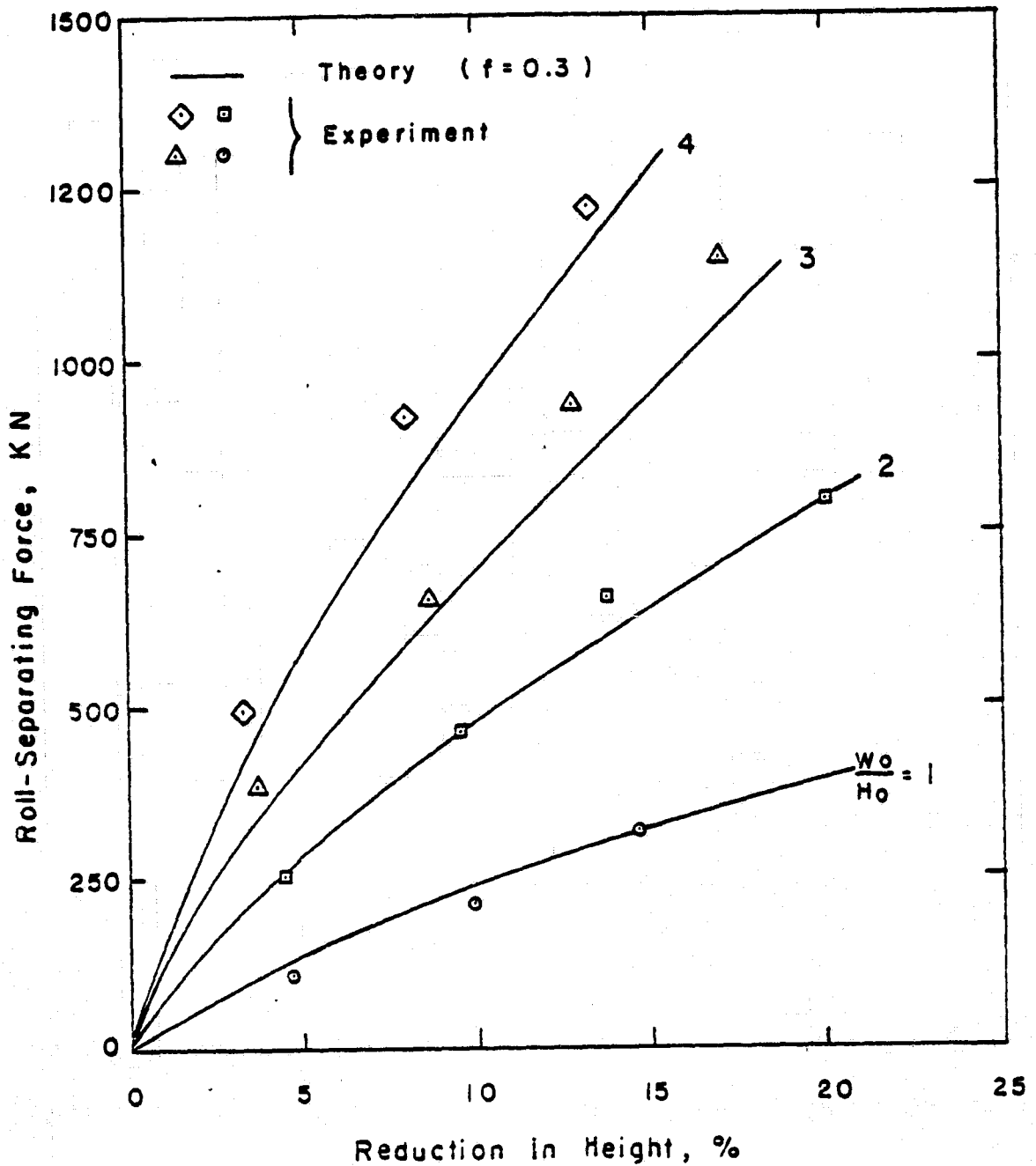


FIGURE 26. THEORETICALLY PREDICTED AND EXPERIMENTALLY MEASURED ROLL-SEPARATING FORCE FOR ROOM TEMPERATURE ROLLING OF 1-INCH THICK MILD STEEL PLATES OF VARIOUS ASPECT RATIO W_0/H_0 (Width/Thickness)

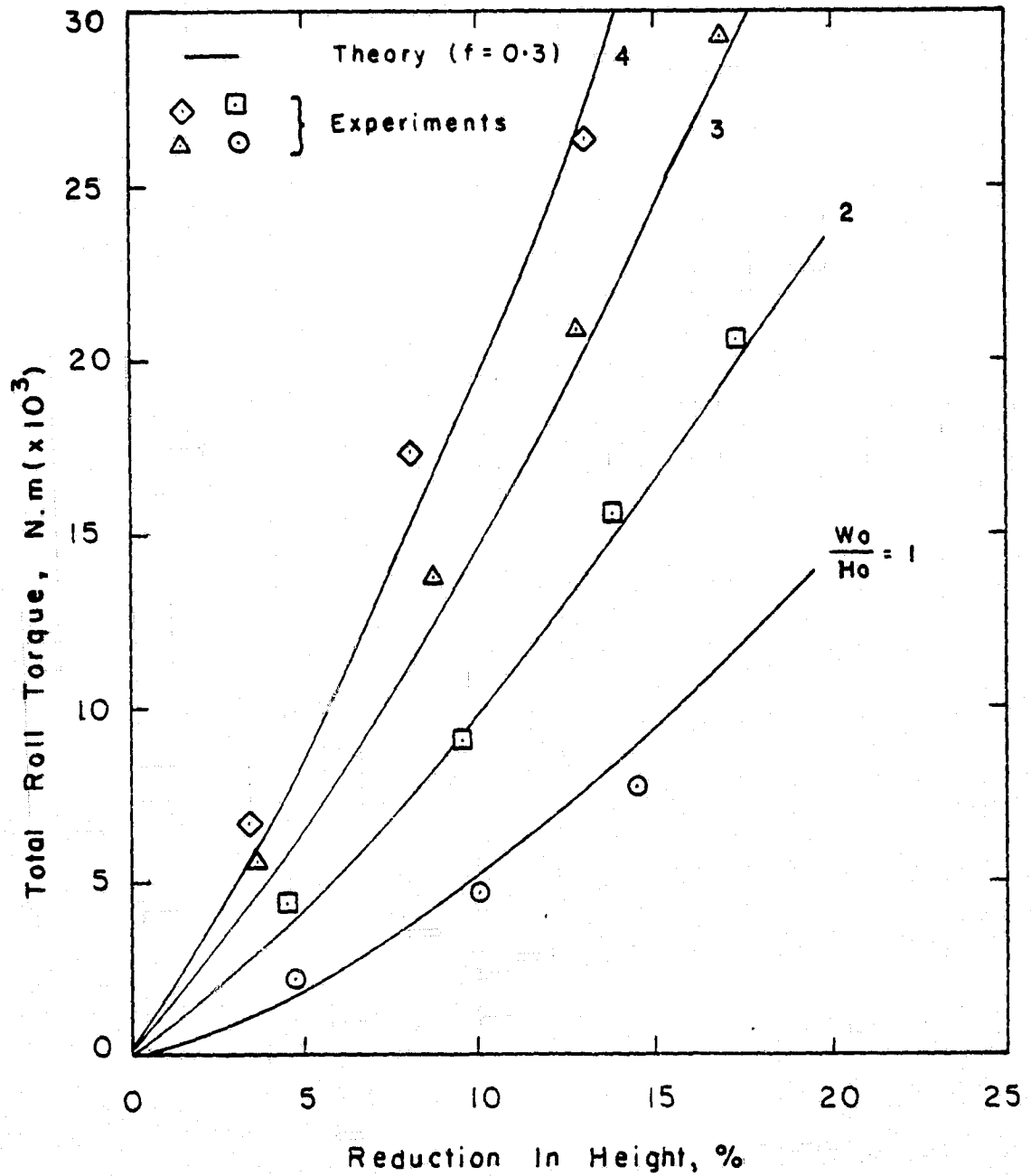


FIGURE 27. THEORETICALLY PREDICTED AND EXPERIMENTALLY MEASURED ROLL TORQUE FOR ROOM TEMPERATURE ROLLING OF 1-INCH THICK MILD STEEL PLATES FOR VARIOUS WIDTH TO THICKNESS RATIOS (W_0/H_0)

Predictions of the lateral spread and roll torque for cold rolling of plates were made by using the computer program SHPROL. Again, the flow stress and the friction data were taken from Task I results. As seen in Figure 28, which shows lateral spread in plate rolling against reduction in height for various width/height ratios of the plates, the agreement between theory and experiment is good at small reductions in height. At large reductions in height, the experimentally measured values of lateral spread are always higher than the theoretically predicted values. This is mainly due to the fact that, at large reductions, the rolls did not bite freely into the plates and a certain amount of axial push was required to accomplish the rolling. Figure 29 shows total roll torque against reduction in height for various widths/height ratios of the plate. The agreement between the predictions and the measurements is reasonably good, except at large reductions for reasons described above.

Similar evaluations of the computer programs ROLPAS and SHPROL under hot-rolling conditions are being conducted currently.

Shape-Rolling Experiments

In order to evaluate the computerized models of shape rolling and roll-pass design, laboratory rolling experiments of an airfoil shape are being planned. For this purpose, a General Electric turbine engine vane (GE, Evendale, Vane for Stator, State 4, Drawing No. 9064M84), as shown in Figure 30, will be cold rolled from mild steel and hot-isothermally rolled from Ti-6Al-4V alloy. The roll shape and pass schedule is being designed by using the computer programs ROLPAS and SHPROL.

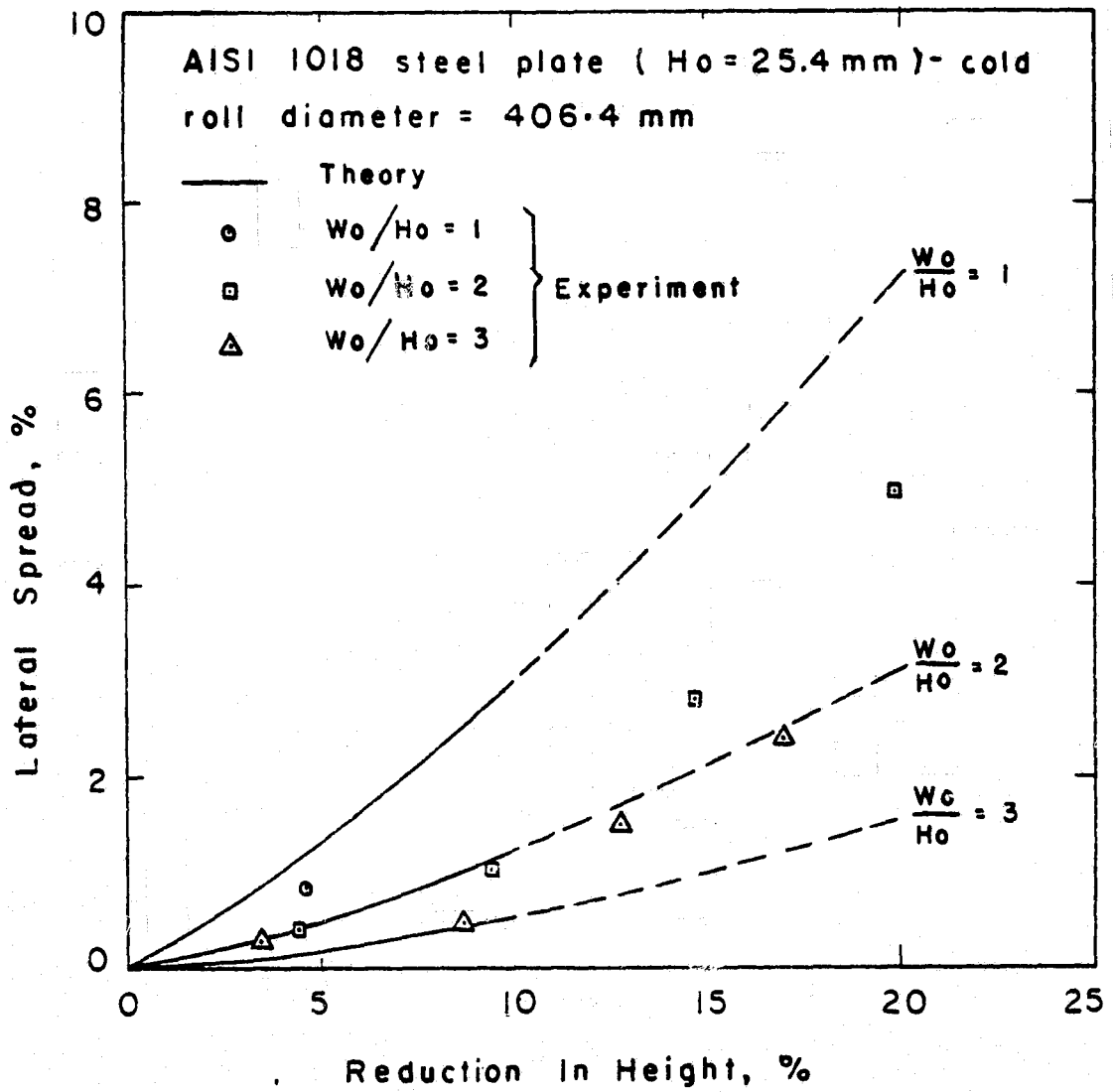


FIGURE 28. THEORETICALLY PREDICTED AND EXPERIMENTALLY MEASURED ROLL TORQUE IN COLD ROLLING OF MILD STEEL PLATES

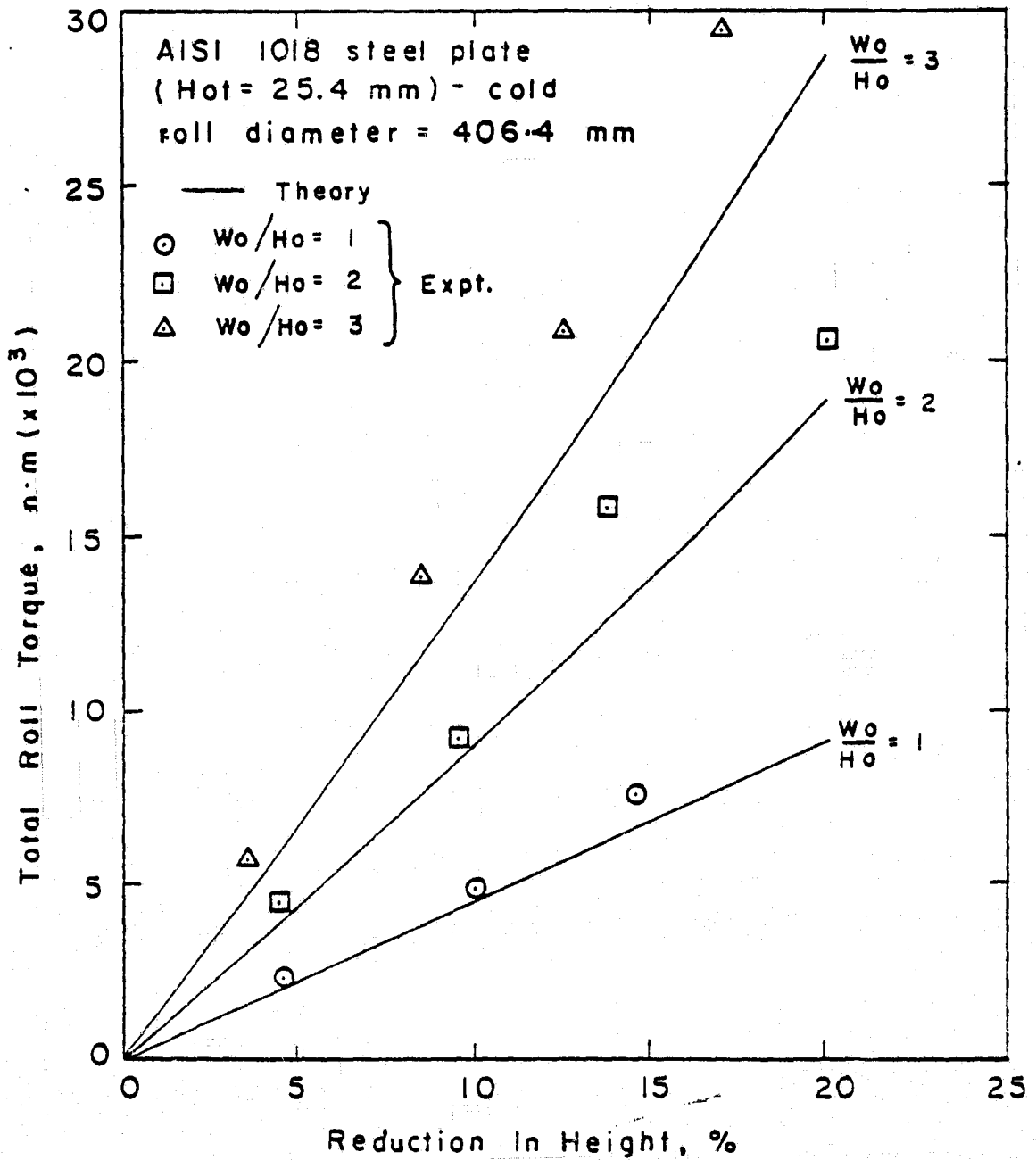


FIGURE 29. THEORETICALLY PREDICTED AND EXPERIMENTALLY MEASURED ROLL TORQUE IN COLD ROLLING OF MILD STEEL PLATES

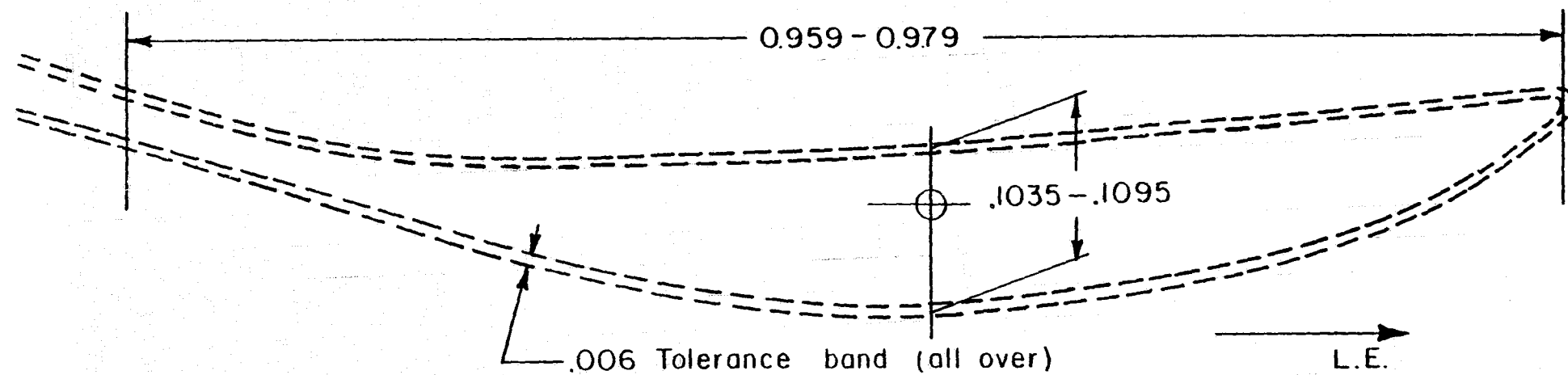


FIGURE 30. THE ENLARGED SKETCH OF THE GE VANE SHAPE, WHICH IS BEING COMMERCIALY ROLLED FROM INCO 718 BY GE-LYNN (This figure has been reduced down from the original 20X mylar drawing supplied by GE)

The laboratory experiments will be conducted on Battelle's two-high rolling mill with 0.203 m (8-inch) diameter x 0.306 m (12-inch) wide rolls (Figure 31). The mill drive is through a 50 hp, 230 V, dc variable speed motor, and the roll surface speed can be varied from 0.33 to 1.02 m/sec (65 to 200 fpm). The rolls consist of tool steel (H13) arbors; the airfoil shape is ground on a pair of sleeves keyed to these arbors, as shown in Figure 32. The sleeves with the airfoil shapes are being made from hardened (R_c 58 to 62) tool steel for cold rolling of mild steel shapes and from IN 100 for hot-isothermal rolling of Ti-6Al-4V shapes. The spacers are being machined and ground from Waspaloy. Thus, the sleeves with airfoil shape will be changed for various shapes and for cold and hot rolling of shapes. In hot-isothermal rolling, the sleeves with airfoil shape will be heated with induction coils wrapped around them, except near the entrance and exit from the rolls.

The rolls are being manufactured currently.

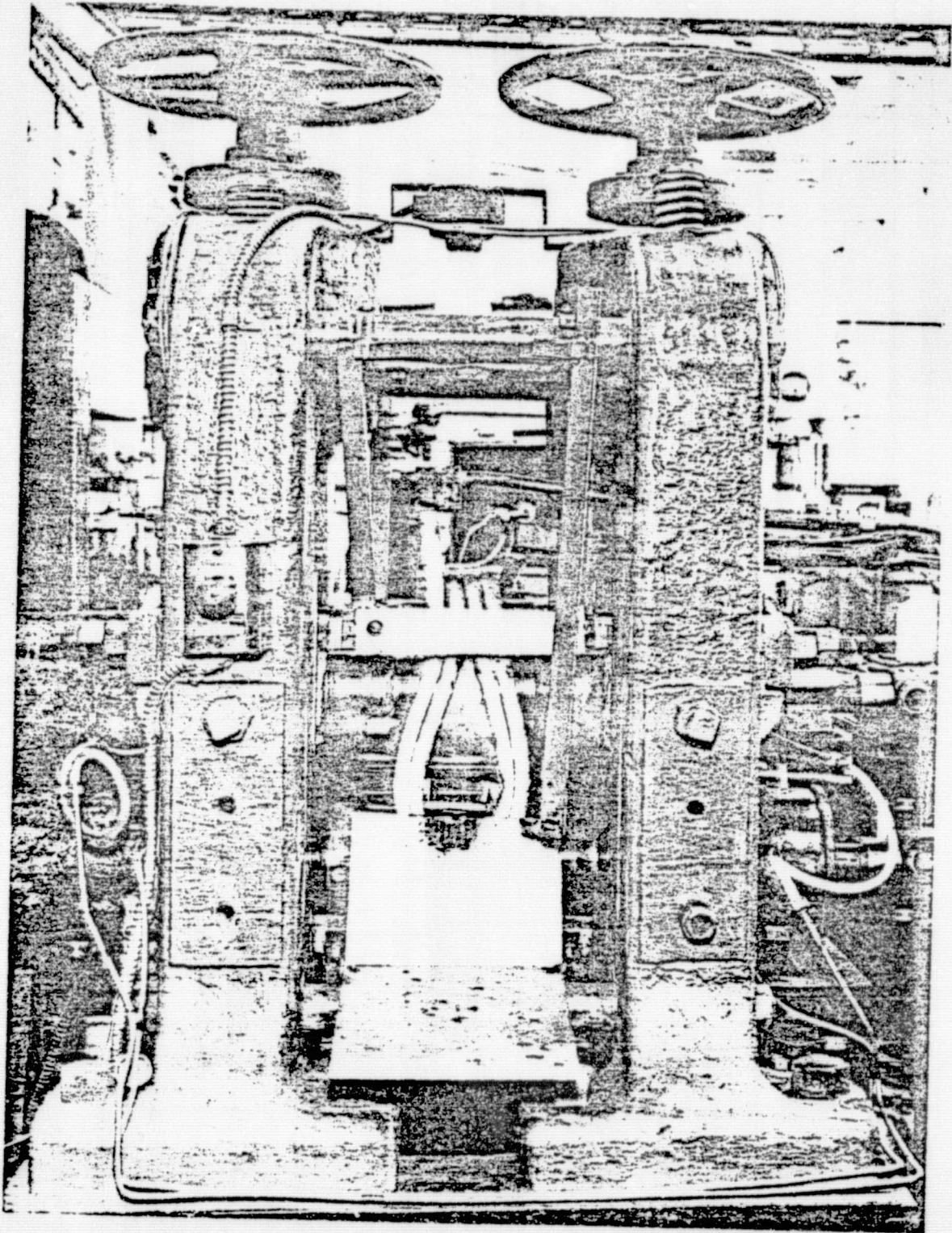


FIGURE 31. EXIT END OF 2-Hi ROLLING MILL FOR ISOTHERMAL SHAPE-ROLLING TRIALS (Induction-Heating Coil Shown in Place)

ORIGINAL PAGE IS
OF POOR QUALITY

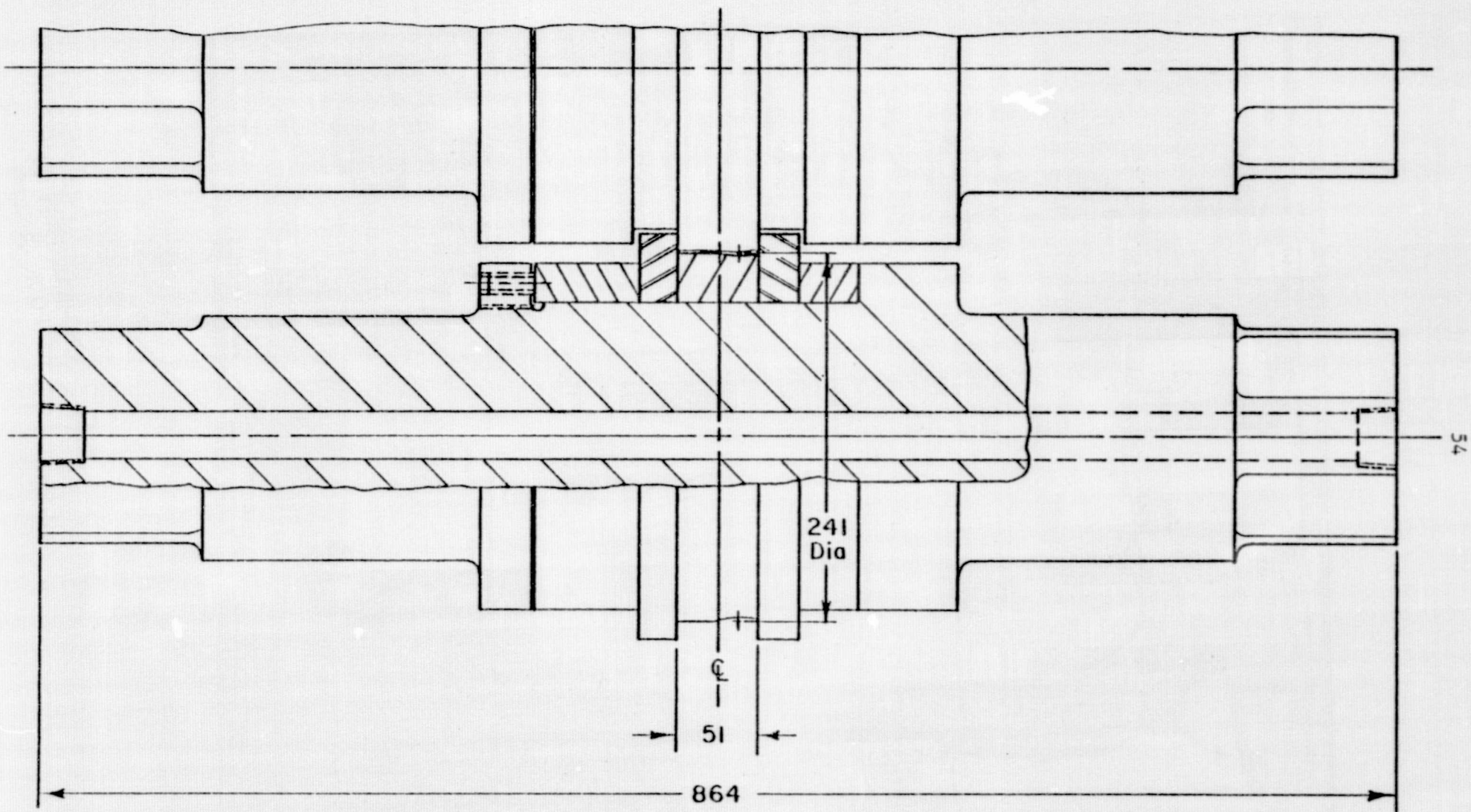


FIGURE 32. ROLL ASSEMBLY FOR ROLLING OF AIRFOIL SHAPES

SUMMARY OF RESULTS AND FUTURE WORK

Rolling of shapes is one of the least understood metal-deformation processes. The factors influencing the shape-rolling process are intermixed and complex so that roll and roll-pass design have been traditionally a purely empirical, intuitive, and experienced-based art. The purpose of this program is to develop and verify a computer-aided method for roll-pass design in rolling airfoil shapes used in engine manufacturing.

A computer-aided design (CAD) system has been developed. This system consists of (a) a mathematical model for predicting metal flow (elongation and spread) in shape rolling, and (b) a model for estimating stresses in rolling and for simulating the rolling process. These models utilize the upper-bound method and the slab method of analysis, respectively. This CAD system requires information on material flow stress and workability and information on interface friction as inputs. The predictions from the CAD system are being verified with respect to cold and hot-isothermal rolling of an airfoil shape. Finally, the cost-benefits of using CAD in general and as applied to rolling of airfoil shapes are being investigated.

This progress report covers (a) the determination of the flow stress, friction and workability data, (b) the development of the CAD system for rolling of airfoil shapes, (c) the evaluation of the CAD system using plate-rolling experiments, and (d) an outline of the shape-rolling experiments to be conducted. The future work will consist of completing the cold and hot-isothermal rolling trials, evaluating the CAD system, and developing a cost-benefit analysis of using CAD in metal-forming process design. A Final Report will be issued upon completion of this program.

REFERENCES

- (1) Trinks, W., Roll-Pass Design, Volumes I and II, The Penton Publishing Company, 1941.
- (2) Beynon, R. E., Roll Design and Mill Layout, Association of Iron and Steel Engineers, Pittsburgh, Pennsylvania, 1956.
- (3) Hoff, E. H., and Dahl, T., Rolling and Roll-Shape Design, (in German) Verlag Stahleisen, Dusseldorf, 1954.
- (4) Neumann, H., Shape Design of Rolls, (in German) VEB Deutscher Verlag, Leipzig, 1969.
- (5) Kruger, C. M., Considerations on the Theory and Practice of Roll-Pass Design, (in German) Stahl und Eisen, 81, 1961, p 858.
- (6) Schutza, A., Comparison of Practical Roll-Pass Designs for Angles, (in German) Stahl und Eisen 90, 1970, p 796.
- (7) Rheinhausen, H. K., and Menne, H., Different Roll-Pass Designs for U Profiles, (in German) Stahl und Eisen, 90, 1970, p 801.
- (8) Wusatowski, Z., The Average Elongation in Shape Rolling, (in German) Neue Hutte, 2, 1957, p 24.
- (9) Neumann, H., Division of a Profile Into Components in Rolling of Steel I-Beams, (in German) Neue Hutte, 1, 1962, p 480.
- (10) Douglas, J. R., Altan, T., and Fiorentino, R. J., "Isothermal Uniform Compression Test for Determining Flow Stress of Metals at Forging Temperature", Chapter 3, A Study of Mechanics of Closed-Die Forging, Phase II, Final Report, (1972) AMMRC-CTR 72-25, Contract No. DAAG46-71-C0095.
- (11) Kobayashi, S., Lee, C. H., and Oh, S. I., "Workability Theory of Materials in Plastic Deformation Processes", USAF Technical Report AFML-TR-73-192, May 1973.
- (12) Burgdoff, N., "Investigation of Friction Values for Metal-Forming Processes by Ring Compression Method", (in German), Industrie-Anzeiger, Vol. 89, 1967, p 799.
- (13) Lee, C. H., and Altan, T., "Influence of Flow Stress and Friction Upon Metal Flow in Upset Forging of Rings and Cylinders", ASME Transactions, J. Engr. Ind., Vol. 94, No. 3, August 1972, p 775.
- (14) Metals Handbook, Vol. 7, Eighth Edition, American Society for Metals, Metals Park, Ohio 44073, 1973.
- (15) Luton, M. J., and Sellows, C. M., "Dynamic Recrystallization in Nickel and Nickel-Iron Alloys During High Temperature Deformation", Acta. Met., Vol. 17, 1969, pp 1033-43.

- (16) Private Communication with Mr. Will Hansen, General Electric Company, Lynn, Massachusetts.